Synthesis, Characterization and Applications of Stibonium (III) Cationic Complex.

A Thesis submitted to

Indian Institute of Science Education and Research (IISER), PUNE;

In partial fulfillment of the requirements for the BS-MS Dual Degree Programme

By

Godey Darmika Vagdevi Sree Keerthi

(BS-MS student; Registration No: 20141121)

Under the supervision of

Dr. Shabana Khan

Assistant Professor

Indian Institute of Science Education and Research

Pune, 411008, INDIA.

Certificate

This is to certify that this dissertation entitled, **"Synthesis, Characterization and Applications of Stibonium (III) Cationic Complex"** towards the partial fulfillment of the BS-MS dual degree programme at the Indian Institute of Science Education and Research, Pune represents the research carried out by **Godey Darmika Vagdevi Sree Keerthi** at Indian Institute of Science Education and Research, Pune under the supervision of **Dr. Shabana Khan**, Assistant Professor, Department of Chemistry during the academic year 2018-2019.

Date: 20/03/19
Place: PUNE

Godey Darmika
5th year BS-MS student
IISER, Pune

Dr. Shabana Khan
Assistant professor
Department of Chemistry
IISER, Pune

Declaration

I hereby declare that the matter embodied in the report entitled, **"Synthesis, Characterization and Applications of Stibonium (III) Cationic Complex"** are the results of the research work carried out by me at the Department of Chemistry, Indian Institute of Science Education and Research, Pune, under the supervision of **Dr. Shabana Khan** and the same has not been submitted elsewhere for any other degree.

Date: 20/03/19
Place: PUNE

Godey Darmika
5th year BS-MS student
IISER, Pune

Dr. Shabana Khan
Assistant professor
Department of Chemistry
IISER, Pune

This Thesis is dedicated to my beloved Parents.

Acknowledgements

On successful completion of my thesis report, it is my pleasure to acknowledge the people who have contributed to this work, be it through guidance, encouragement or moral support.

Firstly, I would like to take the opportunity to express my profound gratitude and sincere thanks for my thesis Supervisor, **Dr. Shabana Khan** for her exemplary guidance, encouragement and support she has provided at every stage of this project. Her friendly nature with the students collapsed the barriers and let us to interact with her frankly. Her valuable suggestions helped me to develop my critical thinking and gain experience as an individual experimentalist. Also, I am grateful to my TAC member, **Dr. R. Boomi Shankar**, Associate professor, Department of Chemistry, IISER Pune, for spending his precious time and providing his valuable suggestions and boosting me with his encouragement to do my project.

I would like to express my special thanks for my mentor, Mr. Rajarshi Dasgupta, for guiding me throughout my project with his friendly attitude and for sharing his knowledge and also for his moral support he has provided during hard times of the project. I would also like to mention my special thanks for Dr. Shiv Pal, Ms. Shweta H. and Ms. Nasrina P., for their all time support and help they have provided with no regret. I would also thank my other Lab members, Ms. Nilanjana S., Mr. Javed Md., Ms. Neha K., Ms. Moushaki G., Mr. Ashok J. and Ms. Tejaswini G. for their support. With out my lab members, this project wouldn't have been possible.

I am thankful to IISER Pune Director, Prof. Jayant B. Udgaonkar, Chemistry Chair person, Prof. M. Jayakannan and all the Chemistry department faculties for supporting me in pursuing my dreams at IISER Pune. I also thank the DST Inspire for providing me financial support to carry out my project. I am indebted to all the technical staff members for making my project easier at IISER Pune.

Lastly, I overwhelmingly deliver my gratefulness to my parents, family and friends for their moral support at every point of my life and for helping me overcome all the physical and mental huddles and complete my project.

Table of Contents

List of Schemes

List of Figures

List of Tables

Table of Abbreviations

Notation	Compound Name
[1]	N-phenylpyridine-2-amine
[1]-Cl	Monochloro amino stibane complex
[1]-Cl_2	Dichloro amino stibane complex
$[1]^+OTf^-$	Stibonium cation complex with triflate anion
[1]-Cl_2-aNHC	Dimer antimony complex with I^tBu-NHC
NHC	N-Heterocyclic carbene
I^tBu-NHC	Iso-teritarybutyl NHC
Dipp-NHC	2,6-Diisopropylphenyl NHC
$SbCl_3$	Antimony trichloride
$SbCl_5$	Antimony pentachloride
^nBuLi	n-butyl lithium
TMSOTf	Trimethylsilyl trifluoromethane sulfonate
TMSCN	Trimethylsilyl cyanide
DMAP	4-Dimethylamino pyridine
HBpin	Pinacolborane
anh. $NaSO_4$	Anhydrous Sodium sulfate
P_2O_5	Phosphorus pentoxide
CaH_2	Calcium hydride
MeCN	Acetonitrile
DCM	Dichloromethane
THF	Tetrahydrofuran
$CDCl_3$	Dueterated chloroform
CO_2	Carbon dioxide
SCXRD	Single Crystal X-Ray Diffraction
NMR	Nuclear Magnetic Resonance

1. Abstract:

As a part of our fundamental research interest on the Lewis acid chemistry exhibited by main group Lewis acids, we chose to explore the activity of electron deficient pnictogen cationic species particularly, stibonium cation **[1]$^+$OTf-**. In objective to synthesize **[1]$^+$OTf-**, initially we successfully synthesized two different precursors, monochloro amino stibane complex, **[1]-Cl** and dichloro amino stibane complex, **[1]-Cl$_2$.** Utilizing **[1]-Cl**, we successfully synthesized its respective cationic complex, **[1]$^+$OTf-**. This **[1]$^+$OTf-** was further utilized to exploit its reactivity and catalytic activity. Based on crystallographic evidence, it was revealed that **[1]$^+$OTf-** is less likely to coordinate with weak donors like MeCN. Additionally, NMR spectroscopic studies of the preliminary catalytic reactions revealed that **[1]$^+$OTf-** is capable of acting as a catalyst for simple organic transformation reactions like hydroboration and cyanosilylation for aldehydes. On the other hand, we also made use of **[1]-Cl$_2$** to generate its respective stibonium cationic and treated it with I^{t}Bu-NHC but surprisingly a dimer complex with Sb-O-Sb bridge connecting two abnormal centers of I^{t}Bu-NHC was obtained which is against the consensus yet an interesting species to carry out further investigative studies.

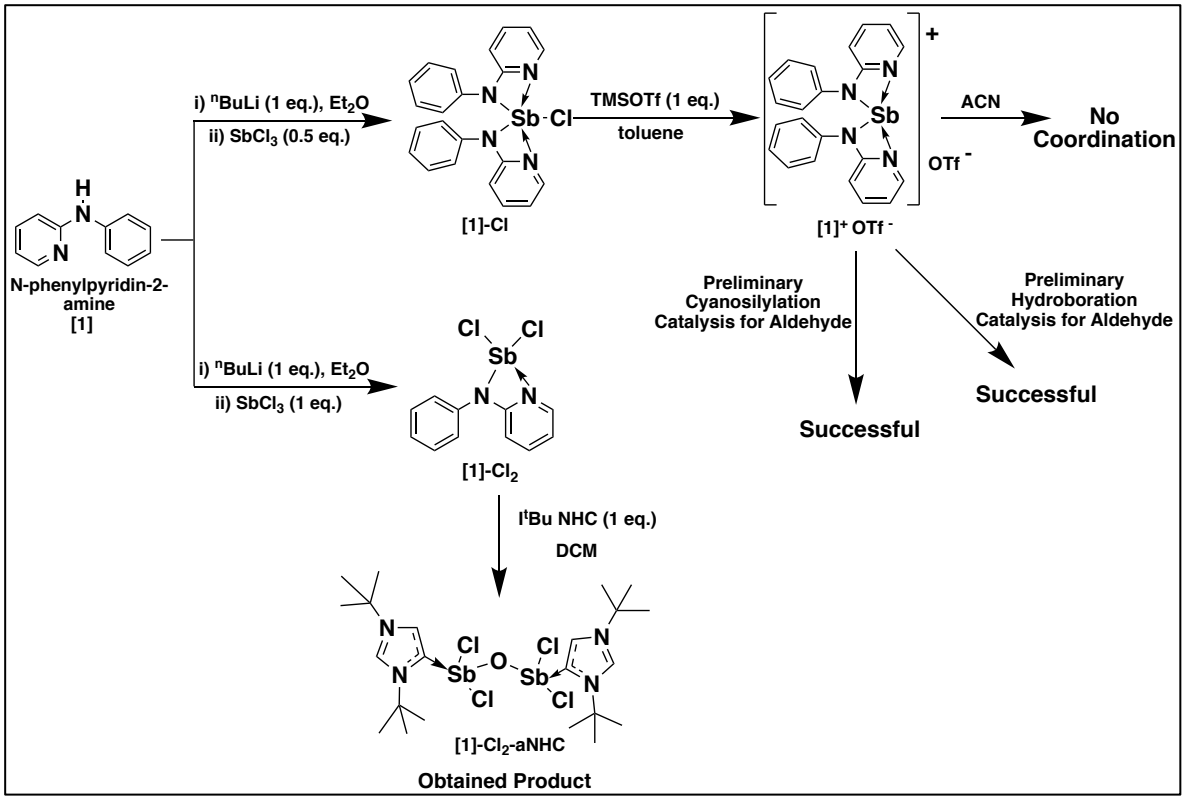

Scheme 1: Schematic representation of the overall synthesis in this thesis work.

2. Introduction:

Over the past few decades, the field of Lewis acid chemistry has grabbed much attention in catalysis as well as in activation of small molecules. It has been conventionally believed that the transition-metal catalysts have been dominant in the field of molecular transformation catalysis for the past many decades especially, the late transition-metal catalysts like complexes based on Rh, Ru, Ir, Pd, Pt, Os, etc. However, the development of novel main group element-derived Lewis acidic complexes that exhibit parallel characteristics and reactivity as that of transition metals, have garnered tremendous attention. With their significant evolution, they have entered into a renaissance in the recent years. There have been many novel s-block and p-block element-based complexes developed that are indefinitely stable at ambient temperatures even in low-valent oxidation state. Amongst these complexes, the properties of pnictogen-based coordination Lewis acidic complexes offered more opportunity for their emergence and allured great interest for exploring their reactivity and catalytic applications. “The pioneering work of Olah also shows that, apart from group 13 and 14 species, the strong Lewis acidity can also be expressed by group 15 elements, especially antimony”,[(1)] as stated by Gabbai *et. al*.[(2)]

Out of various Lewis acidic pnictogen-based cationic complexes, the intrinsically higher Lewis acidity of stibonium cations had allowed them to emerge as powerful Lewis acids and paved way for their drastic exploration in Lewis acid chemistry by many main-group chemists for the past few years. Although, antimony halides (such as $SbCl_3$ and $SbCl_5$) themselves are strong Lewis acids, they are highly reactive and corrosive in nature,[(3)] therefore they couldn’t be utilized extensively as they can complicate their use in organic chemistry. Therefore, scientists thought of developing Lewis acidic antimony cationic derivatives that are decorated with diverse variety of organic ligands, as mentioned by Hudnall *et. al.*[(4)] and Gabbai *et. al.*[(2)] These developed antimony cationic derivatives are relatively easier to handle unlike antimony halides and also the generation of the electron-deficient cationic center enhances its Lewis acidity as compared with that of it’s respective precursor, metal-halide complex.[(5)]

There are many interesting works that have been reported on stibonium cationic complexes and their applications (Table **1** and Table **2**). Earlier studies showed that, stibonium cations can catalyze cycloaddition reactions like addition of isocyanates to epoxides.[(6)] Recent studies showed that, stibonium cations were utilized as catalyst in various organic transformation

reactions like Aldol condensation,[4] Hydrosilylation,[7] Acetalisation,[8] Friedel-Crafts acylation,[9] Michael addition[10] and various other reactions. It was found that stibonium cations can even promote polymerization reactions.[11] Additionally, it was also proven that some Lewis acidic stibonium cations were employed for capturing environmentally toxic anions like fluoride, cyanide and azides.[12, 13] Also, there are few reports which show the activity of stibonium cations as a fluorescent species.[14, 15]

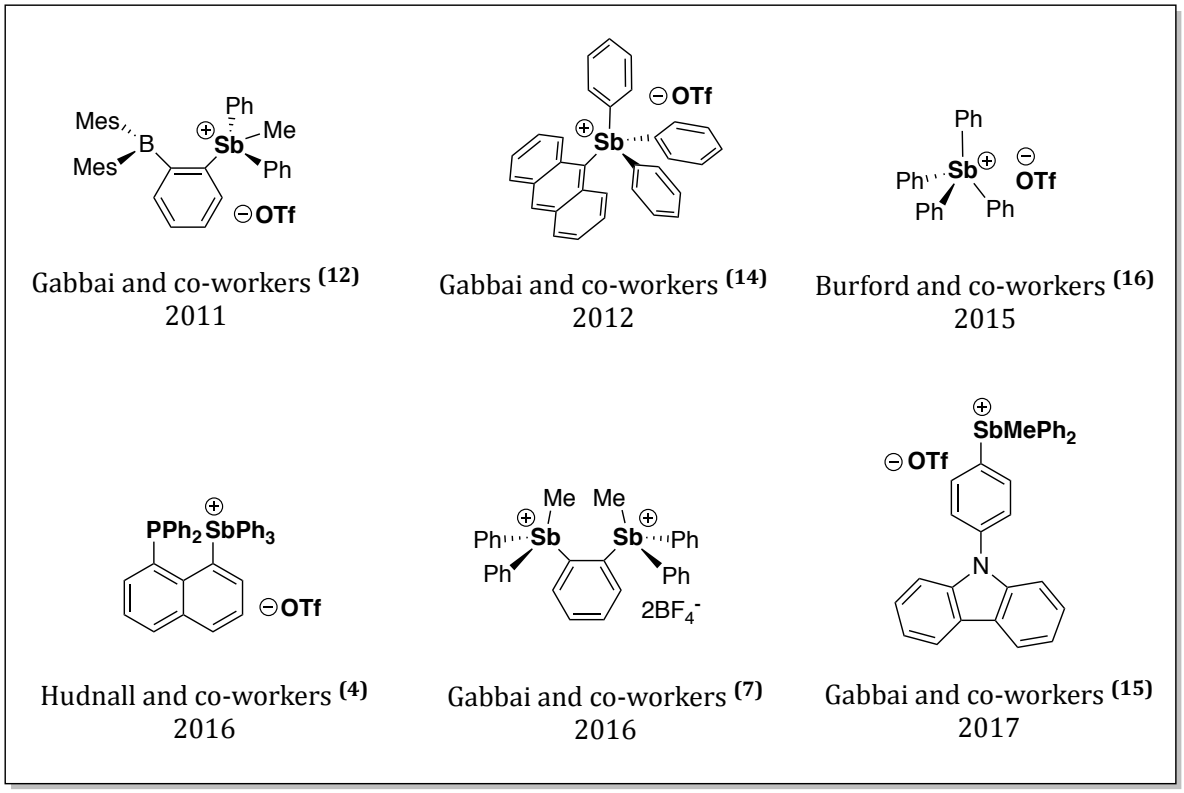

Table 1: List of some examples for stibonium (V) cationic complexes that are recently reported.

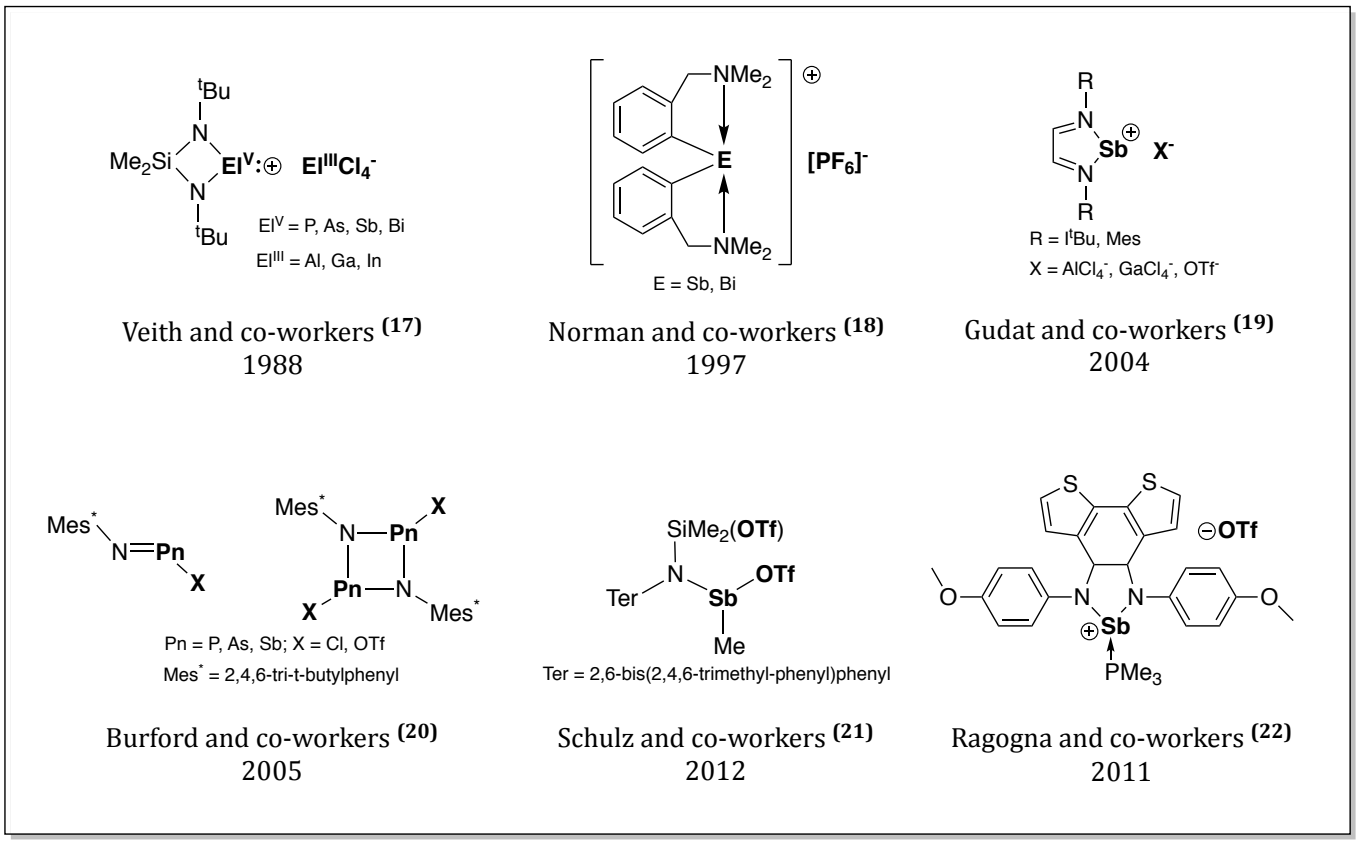

Table 2: List of some examples for stibonium (III) cationic complexes that were reported.

In general, most of the stable stibonium complexes are either in +3 or +5 oxidation state with some exceptions. Till date, a plethora of Sb(V) cationic complexes have been synthesized and its applications were reported as compared to that of Sb(III) cationic complexes relatively. To the best of our knowledge, out of the reported Sb(III) cationic complexes, the complexes that are stabilized by **N**-based ligand system are either cyclic complexes or acyclic complexes that are supported by highly bulky **N**-based ligand system. Also it is noteworthy that, there prevail very limited reports, which shows the catalytic activity of stibonium (III) cationic complexes in any organic transformation reaction. Motivated by the various pioneering on-going research and the limitation in the reports of Sb(III) cationic complexes, our group was highly interested to synthesize a new amino-ligand supported Sb(III) cationic Lewis acidic complex that is acyclic in structure and explore it's reactivity along with its catalytic activity as a part of my thesis project.

Theoretically, multi-dentate ligands are known to provide more chelation thereby, stabilizing the low-valent metal ionic center. Additionally, the most versatile use of the ligand systems with one or more **N**-donor centers in the synthesis of many novel complexes,[23] had enticed us to kick-

start our project with the synthesis of a simple bidentate **N, N'**-donor ligand, N-phenylpyridin-2-amine **[1]**. This ligand is highly stable in open air at ambient temperature and can be synthesized easily (scheme **2***)*. In objective to synthesize the target stibonium (III) cationic complex, we focused to synthesize and isolate the precursors, **[1]-Cl** and **[1]-Cl_2**. By utilizing **[1]** as our primary starting material we synthesized monochloro amino stibane complex, **[1]-Cl** (scheme **3**) and confirmed it with the help of crystallographic evidence (Fig. **1**) and NMR spectroscopic evidences (Fig. **7, 8***).* Further, we treated the isolated **[1]-Cl** complex with TMSOTf to generate its respective stibonium cationic species, **[1]$^+$OTf-** (scheme **4**), which is stable at room temperature. The crystallographic evidence (Fig*.* **3**) and NMR spectroscopic evidence (Fig. **11, 12, 13**) confirmed the formation of **[1]$^+$OTf-**. Initially, we were fascinated to explore the reactivity of the isolated **[1]$^+$OTf-** complex, so we carried a coordination reaction with MeCN as donor but observed no coordination (scheme **7**). Later, we thought of using some better donor than MeCN and therefore, we chose DMAP and N-heterocyclic carbene (Dipp-NHC) as the donors and carried out two different reactions where **[1]$^+$OTf-** was treated with DMAP in one reaction (scheme **8**) and with N-heterocyclic carbene (Dipp-NHC) in another reaction (scheme **9**) but unfortunately we obtained no desired results from both the reactions. Apart from the reactivity, we were also eager to explore the catalytic activity of **[1]$^+$OTf-**, so we set up preliminary catalytic check reactions for hydroboration (scheme **10**) and cyanosilylation (scheme **11**) with **[1]$^+$OTf-** as the catalyst and benzaldehyde as the model substrate. Based on NMR spectroscopic results (Fig*.* **16, 17, 18**), we found that the catalytic transformation for benzaldehyde had taken place successfully with reasonably good yield of 90% and 87% for hydroboration and cyanosilylation respectively. This guarantees its further usage as catalyst in various organic reactions.

Parallelly, we also synthesized the other precursor, dichloro amino stibane complex **[1]-Cl_2** (scheme **5**) by keeping the ligand system unaltered. Crystallographic (Fig. **2**) and NMR spectroscopic results (Fig. **9, 10**) confirmed the **[1]-Cl_2** complex formation. Being aware that there are very limited reports on dicationic stibonium species, we utilized **[1]-Cl_2** complex and made efforts to synthesize its respective dicationic species by treating it with 2 equiv. of TMSOTf but we couldn't isolate the desired product (scheme **13**). In order to provide stabilization to the dicationic species by some external donors, we designed two different reactions where we utilized MeCN (scheme **14**) and DMAP (scheme **15**) as the donors in the two reactions respectively. Unfortunately, here also we didn't obtain the desired product. Later, we treated **[1]-Cl_2** with 1 equiv. of N-heterocyclic carbene (I^tBu-NHC) to obtain the monocationic

species (scheme **12**). Surprisingly, the crystallographic results (Fig. **4**) revealed that an interesting dimer complex is obtained with an Sb-O-Sb bridge connecting the two abnormal centres of I^{t}Bu-NHC, **[1]-Cl$_2$-aNHC**. Though **[1]-Cl$_2$-aNHC** is not the desired product, this complex can be further utilized for investigating the factors responsible for this 'abnormal' mode of binding to the metal-centre and predict the possible mechanism pathway.

3. Experimental Section:

3.1 **Materials:** 2-bromopyridine, n-butyllithium (^{n}BuLi), antimony trichloride ($SbCl_3$), trimethylsilyl trifluorometanesulfonate (TMSOTf), benzaldehyde, 4-dimethylaminopyridine (DMAP), trimethylsilyl cyanide (TMSCN), pinacolborane (HBpin), mesitylene, deuterated chloroform ($CDCl_3$) and anhydrous sodium sulphate (anh. $NaSO_4$) were purchased from Sigma Aldrich chemicals. Acetonitrile (MeCN), diethylether (Et_2O), aniline and tetrahyrofuran (THF) were purchased from Alfa Aesar chemicals. DCM, methanol, acetone were purchased from SDFCL (S D fine-chem. limited). Hexane, toluene and pentane were purchased from AVANTOR limited.

3.2 **General Procedure:** All the reactions were carried out in oven-dried glassware. All the air and moisture sensitive reactions were carried under dried and purified Argon atmosphere by using standard Schlenk-line and dry Glove-box techniques. All the solvents needed for sensitive reactions were purified by distillation over the drying agents (P_2O_5, CaH_2, Na plates and benzophenone) and transferred under Argon prior to use. All the reactions were carried out at room temperature unless mentioned. All the crystals obtained were analyzed by using Single-Crystal X-ray Diffraction (SCXRD). ^{1}H, ^{13}C{^{1}H} and ^{19}F{^{1}H} NMR spectroscopy were carried out in BRUKER/ JOEL NMR spectrophometer at 400 MHz, 100 MHz and 376.6 MHz at 298K respectively with $SiMe_4$ as internal standard and all the chemical shift values are in ppm units. All the NMRs were submitted in $CDCl_3$. HRMS-ESI (High Resolution Mass Spectroscopy Electro-Spray Ionization) was used to characterize the synthesized complexes. All the sensitive samples mass spectroscopy was performed using ultra-pure solvents (UPS).

3.3. Synthesis and Characterization of the Compounds:

3.3.1 Synthesis of N-phenylpyridin-2-amine, [1]:

2-bromo pyridine (3ml, 31.46mmol, 1 equiv.) and aniline (5.74ml, 62.92mmol, 2 equiv.) were taken in a round-bottom flask and kept for heating at 170^{o}C for ~12 hrs under constant stirring (Scheme **2**). Upon cooling, a deep violet colored solid compound was obtained which was dissolved in DCM and washed with brine (saturated NaCl solution). The collected organic layer was dried over anh. $NaSO_4$ and volatiles were removed by using rotary evaporator to obtain the crude product, which was further purified by using column chromatography and re-crystallized in DCM/hexane in 2:1 (v/v) at -30^{o}C. The **[1]** crystals were observed to be colorless with 89% (7.4g) yield.

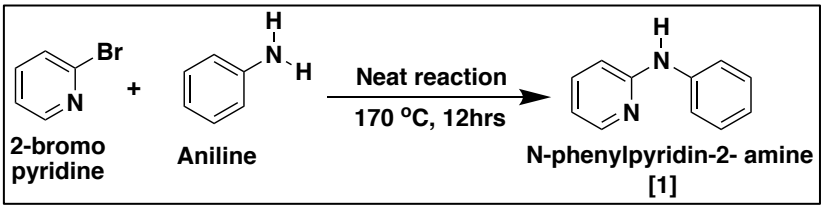

Scheme 2: Schematic representation of synthesis of N-phenylpyridine-2-amine, **[1]**.

^{1}H NMR (400 MHz, $CDCl_3$, δ, ppm): 6.61 (1H, *br-s*, N**H**), 6.72 (1H, *ddd*), 6.88 (1H, *ddd*), 7.04-7.06 (1H, *m*), 7.31-7.33 (4H, *m*), 7.46-7.48 (1H, *m*), 8.20-8.21 (1H, *m*). ^{13}C{^{1}H} NMR (100 MHz, $CDCl_3$, δ, ppm): 108.28, 115.13, 120.44, 122.92, 129.39, 137.80, 140.51, 148.49, 156.07.

3.3.2 Synthesis of monochloro amino stibane complex, [1]-Cl:

N-phenylpyridin-2-amine, **[1]** (2g, 11.75mmol, 1 equiv.) was weighed and transferred to a Schlenk flask and carried out deprotonation under argon by adding a strong base like ^{n}BuLi (1.6M, 11.75mmol, 7.34ml, 1 equiv.) at -78^{o}C in diethylether solution of **[1]** in order to generate it's respective organolithium derivative *in situ*, and let it stir for 4-5 hrs at room temperature. Later, coupling reaction of the corresponding organolithium derivative and $SbCl_3$ (1.34g, 5.875mmol, 0.5 equiv.) was carried out to synthesize **[1]-Cl** (Scheme **3**). The resulting LiCl precipitate was removed via *in situ* filtration in toluene followed by evaporation of volatiles *in vacuo*. Crystallization was also carried in toluene to obtain pale yellow rod-shaped crystals at room temperature with an yield of 62% (1.68g).

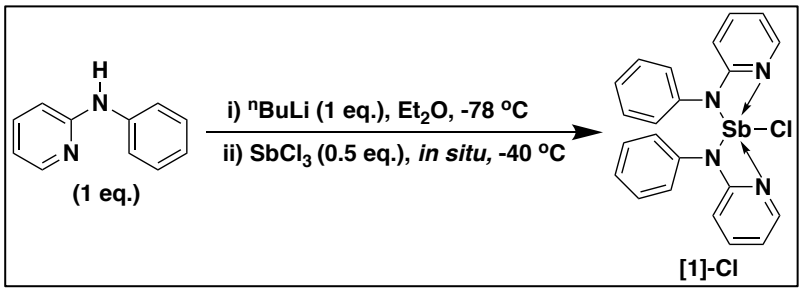

Scheme 3: Schematic representation of synthesis of Chloro-Amino-Stibane complex **[1]-Cl**.

Mp: 160 – 168 ^{o}C. ^{1}H NMR (400 MHz, $CDCl_3$, δ, ppm): 6.11 (2H, *ddd*), 6.54 (2H, *ddd*), 6.68 (4H, *ddd*), 7.12-7.13 (2H, *m*), 7.21-7.22 (4H, *m*), 7.36-7.37 (1H, *m*), 7.95-7.96 (2H, *m*). ^{13}C{^{1}H} NMR (100 MHz, $CDCl_3$, δ, ppm): 107.8, 112.52, 126.07, 128.97, 139.45, 141.49, 144.71, 162.51. ESI-MS (positive) calculated for $C_{22}H_{18}N_4SbCl$: 494.03, found: 494.24.

3.3.3 Synthesis of stibonium cationic complex, $[1]^{+}OTf^{-}$:

A solution of **[1]-Cl** complex (460mg, 0.93mmol, 1 equiv.) was prepared in toluene followed by addition of TMSOTf (0.17ml, 0.93mmol, 1 equiv.) under argon at -78^{o}C to the solution. The reaction mixture was allowed to stir for ~12 hrs at room temperature (Scheme **4**). The resultant solution was filtrated *in situ* and the volatiles were evapourated *in vacuo*. Crystallization was carried out in toluene at room temperature to obtain pale-yellow rod-shaped crystals with yield of 62% (353mg).

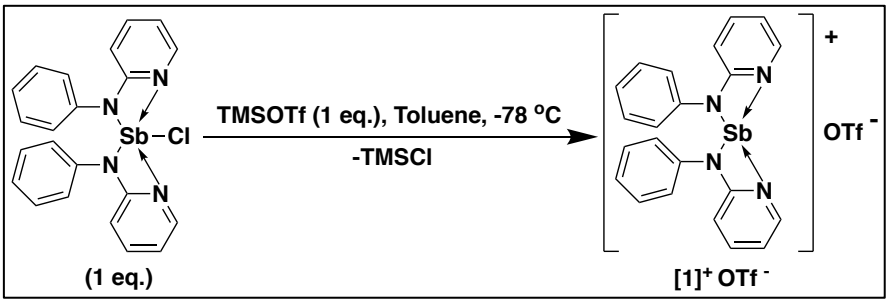

Scheme 4: Schematic representation of generation of stibonium cation **$[1]^{+}$ OTf-** with TMSOTf.

Mp: 105 – 118 ^{o}C. ^{1}H NMR (400 MHz, $CDCl_3$, δ, ppm): 6.88 (2H, *ddd*), 7.08 (2H, *ddd*), 7.20-7.25 (2H, *m*), 7.33-7.34 (4H, *m*), 7.45-7.5 (4H, *m*), 7.75-7.76 (2H, *m*), 8.00-8.01 (2H, *m*). ^{13}C{^{1}H} NMR (100 MHz, $CDCl_3$, δ, ppm): 110.36, 114.15, 123.04, 125.29, 128.22, 129.03, 129.93, 140.63, 142.30. ^{19}F{^{1}H} NMR (376.6 MHz, $CDCl_3$, δ, ppm): -78.39. ESI-MS (positive) calculated for $C_{23}H_{18}N_4SbSO_3F_3$: 608.01, found: 609.08 [M^{+}(608.01)+H].

3.3.4 Synthesis of dichloro amino stibane complex, [1]-Cl_2:

N-phenylpyridin-2-amine, **[1]** (2g, 11.75mmol, 1 equiv.) was weighed and taken in a Schlenk flask to carry out deprotonation of the amine, **[1]** under argon by adding a strong base like ^{n}BuLi (1.6M, 11.75mmol, 7.34ml, 1 equiv.) at -78^{o}C in diethylether soltion of **[1]** in order to generate it's respective organolithium derivative *in situ*, and let it stir for 4-5 hrs at room temperature. Later, coupling reaction of the corresponding organolithium derivative and $SbCl_3$ (2.68g, 11.75mmol, 1 equiv.) was carried out to synthesize **[1]-Cl_2** (Scheme **5**). The resulting LiCl precipitate was removed via *in situ* filtration in toluene followed by evaporation of volatiles *in vacuo*. The compound was allowed to crystallize in toluene at room temperature for overnight to obtain pale yellow block-shaped crystals with an yield of 61% (2.61g).

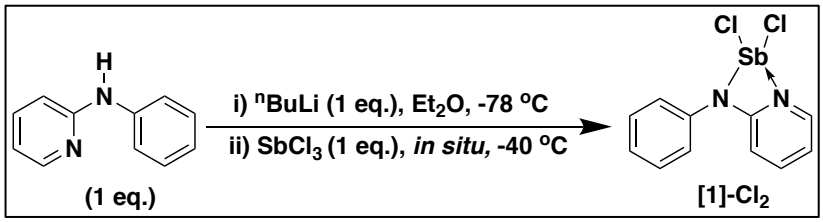

Scheme 5: Schematic representation of synthesis of dichloro amino stibane complex, **[1]-Cl_2**.

Mp: 130 – 138 ^{o}C. ^{1}H NMR (400 MHz, $CDCl_3$, δ, ppm): 6.35 (1H, *ddd*), 6.77 (1H, *ddd*), 7.25-7.27 (2H, *m*), 7.31-7.32 (1H, *m*), 7.47-7.48 (2H, *m*), 7.57-7.58 (1H, *m*), 8.00-8.01 (1H, *m*). ^{13}C{^{1}H} NMR (100 MHz, $CDCl_3$, δ, ppm): 108.26, 114.36, 127.39, 129.39, 139.28, 140.85, 144.02, 162.15. ESI-MS (positive) calculated for $C_{11}H_9N_2SbCl$: 359.92, found: 359.24.

3.3.5 Synthesis of dimer complex from [1]-Cl_2 and ItBu-NHC to obtain [1]-Cl_2-aNHC:

A solution of I^{t}Bu carbene was made in toluene followed by addition of **[1]-Cl_2** to the prepared solution under argon. The reaction mixture was allowed to stir for ~12 hrs at room temperature (Scheme **6**). The solvent toluene was evapourated completely *in vacuo* followed by addition of DCM to solubilize the compound. Later *in* situ filtration was done and all the volatiles were removed *in vacuo*. Crystallization was carried out in DCM/pentane mixture (2:1 v/v) to grow the crystals that are suitable for SCXRD analysis. However, the product obtained, **[1]-Cl_2-aNHC** is unprecedented.

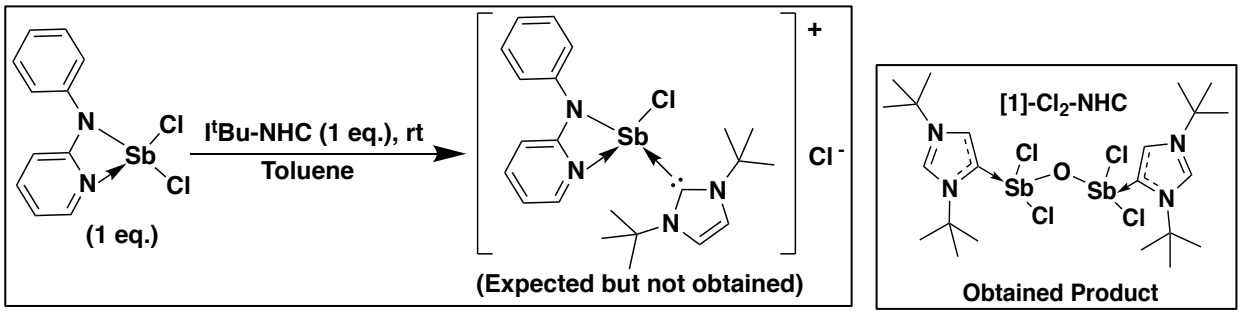

Scheme 6: Schematic representation of the reactivity carried between **[1]-Cl_2** and I^tBu-NHC.

^{1}H NMR (400 MHz, $CDCl_3$, δ, ppm): 1.71 (18H, *s*), 1.84 (18H, *s*), 7.97 (2H, *s*), 8.83 (2H, *s*).
$^{13}C\{^1H\}$ NMR (100 MHz, $CDCl_3$, δ, ppm): 30.21, 31.39, 126.39, 128.21, 129.03, 129.57.

3.4 Exploration on the Applications of the Synthesized Complexes:

3.4.1 Investigation on the reactivity of stibonium (III) cationic complex, $[1]^+OTf^-$:

In aim to investigate the futher reactivity of the synthesized stibonium cationic complex, we set up various reactions as follows:

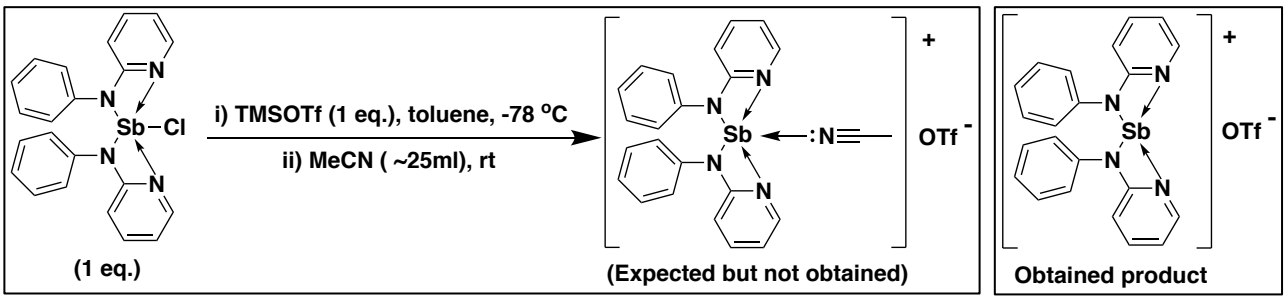

Scheme 7: Schematic representation of the reactivity reaction carried between *in situ* generated **$[1]^+OTf^-$** and MeCN.

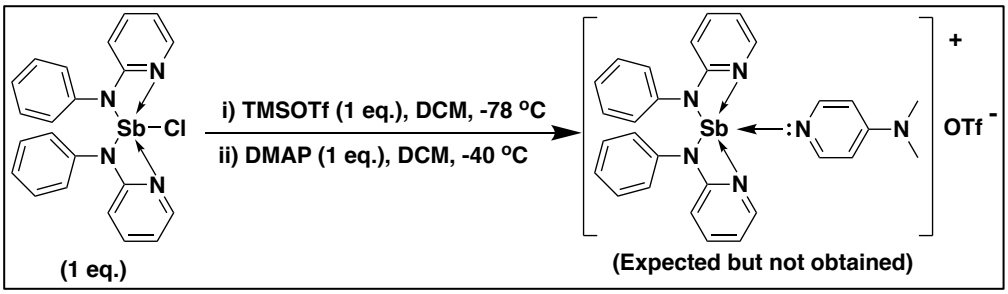

Scheme 8: Schematic representation of the reactivity reaction carried between *in situ* generated **$[1]^+OTf^-$** and DMAP.

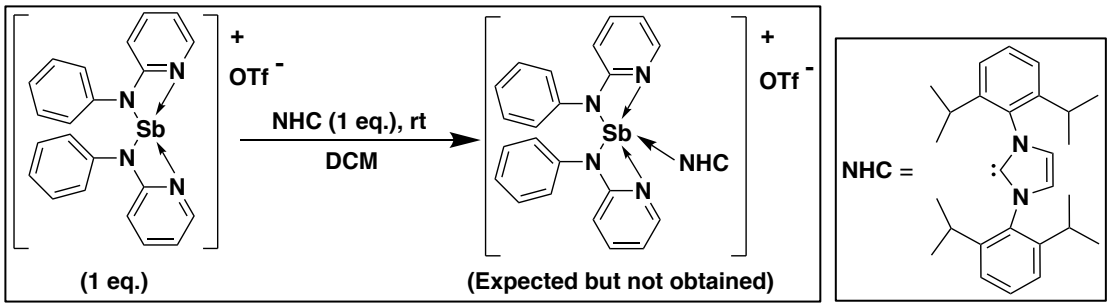

Scheme 9: Schematic representation of the reactivity reaction carried between isolated **[1]$^{+}$OTf-** and Dipp-NHC.

3.4.2 Investigation on the catalytic activity of stibonium (III) cationic complex, [1]$^{+}$OTf- :

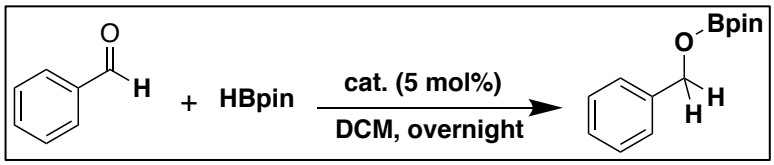

Scheme 10: Schematic representation of the preliminary catalytic reaction of hydroboration of aldehyde with **[1]$^{+}$OTf-** as the catalyst and benzaldehyde as the model substrate.

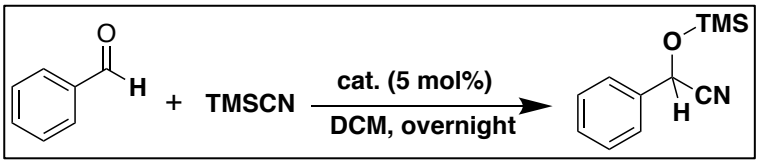

Scheme 11: Schematic representation of the preliminary catalytic reaction of cyanosilylation of aldehyde with **[1]$^{+}$OTf-** as the catalyst and benzaldehyde as the model substrate.

3.4.3. Investigation on the reactivity of dichloro amino stibane complex, [1]-Cl_2:

In aim to investigate the futher reactivity of the synthesized **[1]-Cl_2** complex, we set up various reactions as follows:

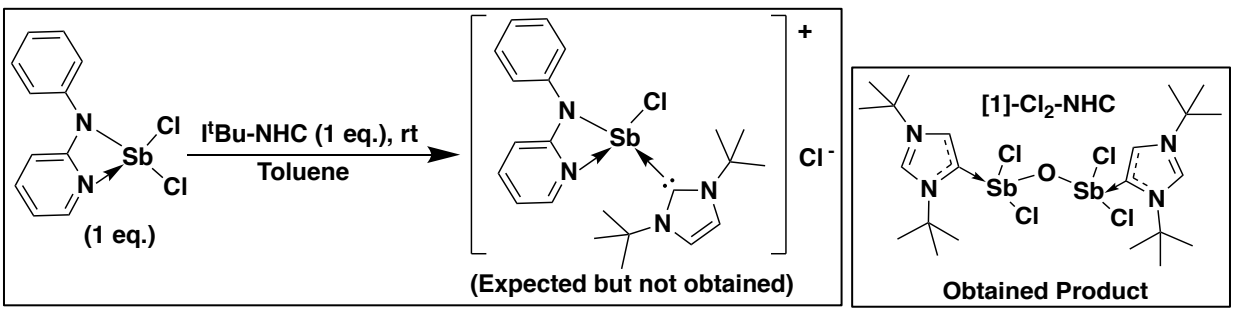

Scheme 12: Schematic representation of the reactivity reaction between **[1]-Cl_2** and I^{t}Bu-NHC to generate monocationic stibonium species.

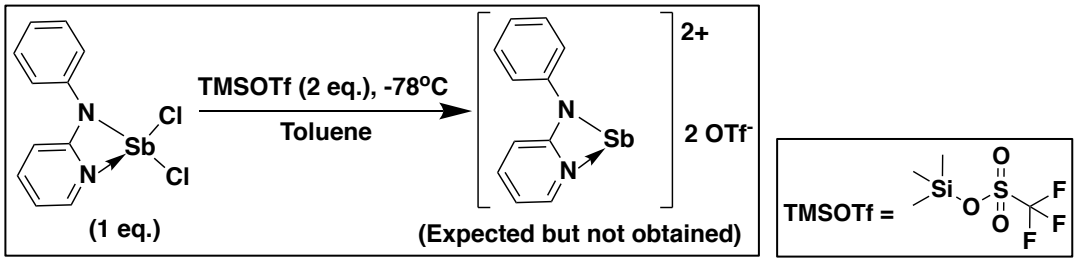

Scheme 13: Schematic representation of the reactivity reaction between **[1]-Cl_2** and TMSOTf to generate dicationic species.

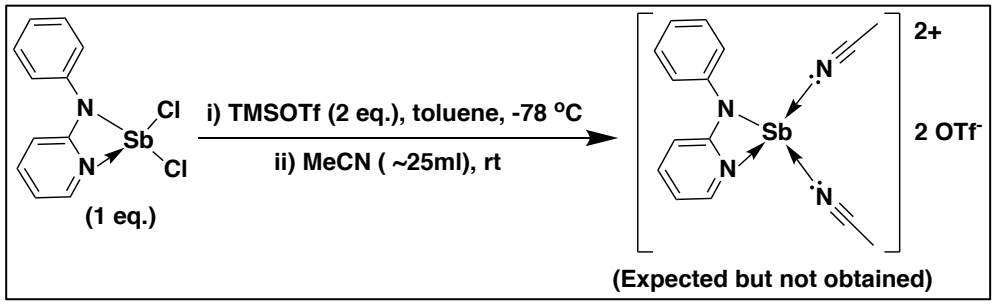

Scheme 14: Schematic representation of reaction carried to stabilize the *in situ* generated dicationic species of **[1]-Cl_2** with MeCN.

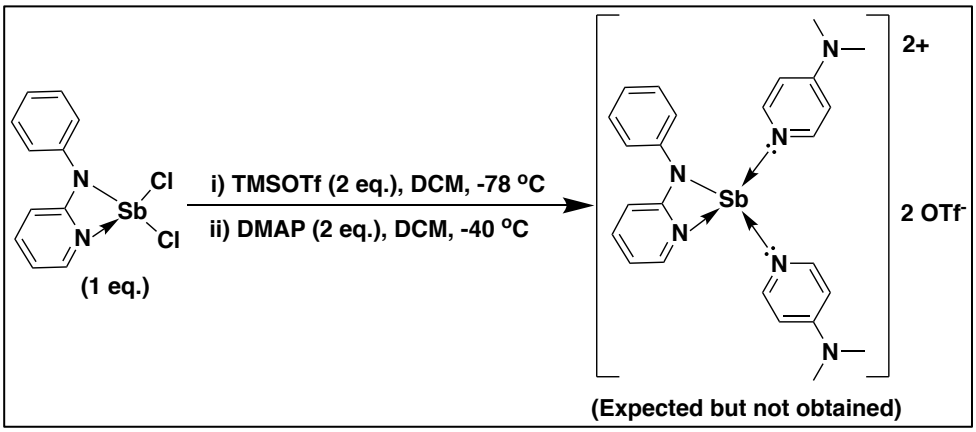

Scheme 15: Schematic representation of reaction carried to stabilize the *in situ* generated dicationic species of **[1]-Cl_2** with DMAP.

None of the above attempted reactions (*schemes **7-15***) resulted in the desired product. And reaction between **[1]-Cl_2** and I^tBu-NHC (*scheme **7***), resulted in an interesting unprecedented dimer complex, **[1]-Cl_2-aNHC**.

4. Results and Discussion:

In interest with the synthetic investigation of Lewis acidic stibonium cationic complex, firstly we synthesized the organic ligand, N-phenylpyridyl-2-amine **[1]** and subjected the obtained compound for NMR spectroscopic study. The NMR results (Fig. **5, 6**) were tallied with it's previously reported NMR data.[24] The appearance of the broad singlet peak at 6.61ppm in the ^{1}H NMR (Fig. **5**) shows the existence of the N-H proton of the secondary amine, **[1]**. Secondly, utilizing this ligand **[1]** we focused to synthesize two different precursors by keeping the ligand system unchanged but by varying the molar equivalent ratio of the ligand **[1]** and $SbCl_3$. The first reaction was set up with 2 eq. of **[1]** and 1 eq. of $SbCl_3$ to synthesize monochloro amino stibane complex, **[1]-Cl**. The obtained crystals of the compound were subjected to X-ray diffraction crystallographic studies and the SCXRD results (Fig. **1**) clearly showed the formation of **[1]-Cl**. The NMR spectroscopic studies (Fig. **7, 8**) also served as supporting evidence. The disappearance of the broad singlet N-H peak of **[1]** in the ^{1}H NMR of **[1]-Cl** (Fig. **7**), reveals that the starting material **[1]** was completely consumed in the formation of **[1]-Cl**. In the second reaction, 1 eq. of **[1]** and 1 eq. of $SbCl_3$ were taken to synthesize **[1]-Cl$_2$**. The obtained crystals of the compound were subjected for SCXRD crystallographic analysis and NMR spectroscopic studies. The SCXRD results (Fig. **2**) clearly showed the formation of the desired product, **[1]-Cl$_2$**. Just-like in case of **[1]-Cl**, here also the disappearance of the broad singlet peak in the ^{1}H NMR of **[1]-Cl$_2$** (Fig. **9**) shows that the starting material, **[1]** was completely consumed in the formation of **[1]-Cl$_2$**. Further, the treatment of **[1]-Cl** with TMSOTf resulted in the generation of stibonium cation with OTf^- as the counter anion. The SCXRD analysis of the obtained **[1]$^+$OTf-** crystals (Fig. **3**) clearly depicted the formation of **[1]$^+$OTf-** with it's molecular structure similar to that of the theoritically predicted product. The absence of the broad singlet peak in the ^{1}H NMR of **[1]$^+$OTf-** (Fig. **11**), tells that there is no hydrolysis of **[1]$^+$OTf-** and the presence of intense singlet peak at -78.4 ppm in the ^{19}F{^{1}H} NMR of **[1]$^+$OTf-** (Fig. **13**) which is within the peak range (-60ppm to -80ppm) of R-CF_3 moeity tells the presence of the counter anion, **OTf-** (triflate anion) that is bound to the cationic counter part of **[1]$^+$OTf-** which is also evident from the SCXRD results (Fig. **3**). Later, 1 eq. of the synthesized **[1]-Cl$_2$** was treated with 1 eq. of I^{t}Bu-NHC in order to generate its respective monocationic complex. The obtained crystals were subjected to crystallographic study and the results (Fig. **4**) revealed that we did not get the desired cationic complex but rather we obtained an interesting dimer product with two abnormal I^{t}Bu-NHCs bridged by Sb-O-Sb

bond. In general, NHCs bind to the metal centre via "normal" binding mode (M-$C1_{carbene}$ binding) but due to various factors NHCs sometimes tend to isomerize and prefer for "abnormal" or "mesoionic" binding mode (M-$C2_{carbene}$ or M-$C3_{carbene}$ binding) with proton migration to the $C1_{carbene}$ centre (Fig. **4**) and migration of the electron pair on to $C2_{carbene}$ or $C3_{carbene}$ centre.[25] This extra mode of binding of NHCs had actually increased their versatile use and there are chemists who solely focused on studying these abnormal carbenes.[25, 26] Since we have unexpectedly obtained **[1]-Cl_2-aNHC** which, is an interesting dimer complex with abnormal binding of NHC, its possible mechanism and the factors responsible for this 'abnormal' mode of binding will be studied in future.

On the other hand, in order to check the catalytic activity of **[1]$^+$OTf-**, a preliminary catalytic hydroboration reaction was set up by utilizing 5mol% of **[1]$^+$OTf-** as the catalyst, benzaldehyde as model substrate and DCM as solvent. The obtained product was thoroughly dried *in vacuo* and subjected for NMR spectroscopic study by taking mesitylene as the internal standard. The peak at 4.94ppm of the resultant ^{1}H NMR (Fig. **14**) clearly showed the conversion of benzaldehyde to its respective boroester with an appreciable yield of 90%. Similarly, we also carried out a preliminary catalytic cyanosilylation reaction with same experimental conditions and subjected the obtained product for NMR spectroscopic study. The peaks at 5.55ppm in ^{1}H NMR (Fig. **15**) and 63.78ppm in the $^{13}C\{^1H\}$ NMR (Fig. **16**) clearly shows the conversion of benzaldehyde to its respective cyanosilylated derivative form with an appreciable yield of 87%.

4.1. Crystallographic Evidences:

	[1]-Cl	**[1]-Cl_2**	**[1]$^+$ OTf$^-$**	**[1]-Cl_2-aNHC**
Chemical formula	$C_{22}H_{18}N_4SbCl$	$C_{11}H_9N_2SbCl_2$	$C_{23}H_{18}N_4SbSO_3F_3$	$C_{22}H_{40}Cl_4N_4OSb_2$
Formula weight	495.62 g/mol	361.87 g/mol	609.24 g/mol	761.91 g/mol
Temperature	150(2) K	150(2) K	150(2) K	150(2) K
Wavelength	0.71073 Å	0.71073 Å	0.71073 Å	0.71073 Å
Crystal system	Triclinic	Triclinic	Monoclinic	Monoclinic
Space group	P -1	P -1	P c	C 2/c
Unit cell lengths	a = 8.7014(11) Å	a = 9.484(4) Å	a = 10.130(2) Å	a = 15.748(7) Å
	b = 9.1248(12) Å	b = 10.342(4) Å	b = 12.250(3) Å	b = 13.636(6) Å
	c = 13.8189(17) Å	c = 13.520(5) Å	c = 12.040(3) Å	c = 16.358(7) Å
Unit cell angles	α = 106.932(3) °	α = 100.030(7) °	α = 90°	α = 90°
	β = 106.791(3) °	β = 95.861(7) °	β = 102.452(2) °	β = 100.99(2) °
	γ = 92.111(4) °	γ = 102.601(7)°	γ = 90°	γ = 90°
Volume	996.083 Å^3	1260.76 Å^3	1458.93 Å^3	3448.29 Å^3
Z	2	4	1	8

Table 3: Crystallographic data for **[1]-Cl**, **[1]-Cl_2**, **[1]$^+$ OTf$^-$**, and **[1]-Cl_2-aNHC**.

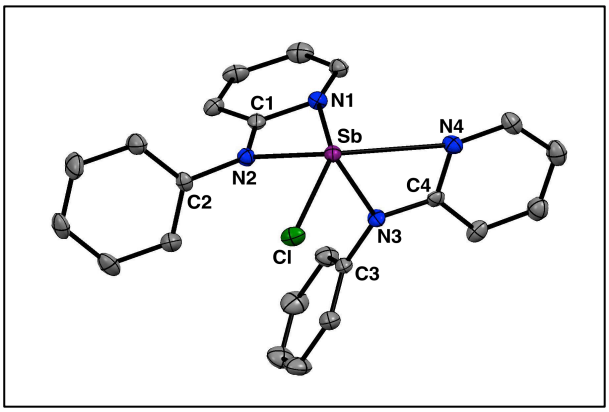

Fig. 1: Molecular structure of **[1]-Cl** in ORTEP representation with 50% displacement ellipsoids as shown (hydrogen atoms and few carbon labeling are omitted for clarity).

Bond lengths	(Å)	Bond angles	(°)
Sb-Cl	2.463	N2-Sb-Cl	90.02
Sb-N1	2.468	N3-Sb-Cl	88.61
Sb-N2	2.088	N1-Sb-Cl	126.53
Sb-N3	2.087	N4-Sb-Cl	126.53
Sb-N4	2.742	N1-Sb-N2	53.97
N2-C1	1.371	N2-Sb-N3	93.40
N2-C2	1.423	N3-Sb-N4	58.07
N3-C3	1.440	N1-Sb-N4	74.63
N3-C4	1.354	C1-N2-C2	120.29
		C3-N3-C4	120.03

Table 4: List of specific bond lengths and bond angles of **[1]-Cl** molecule in angstrom and degree units respectively.

The **[1]-Cl** complex (Fig. **1**) is an Sb(III) complex with a distorted square pyramidal geometry. Here (Fig. **1**), the antimony metal center has five bonds out which three are covalent bonds [Sb-Cl (2.463 Å ~2.4 Å), Sb-N2 (2.088 Å~2.033 Å) and Sb-N3 (2.087 Å~2.033 Å)] and two are coordinate bonds [Sb-N1 (2.468 Å~2.42 Å) and Sb-N4 (2.742 Å~2.42 Å)].[21] On comparing the bond lengths [Sb-N1 = 2.468 Å, Sb-N2 = 2.088 Å, Sb-N3 = 2.087 Å, Sb-N4 = 2.742 Å] (Table **4**), it is clearly evident that Sb-N2 and Sb-N3 covalent bonds have equal bond lengths and these bonds are relatively shorter than the Sb-N1 and Sb-N4 coordinate bonds. Here, the Sb atom is out of the plane containing the four N atoms thereby resulting distortion in the geometry. Considering the bond angles [Cl-Sb-N1 = 126.53°, Cl-Sb-N2 = 90.02°~90°, Cl-Sb-N3 = 88.61°~90°, Cl-Sb-N4 = 126.53°] (Table **4**), it is clear that the Sb-Cl bond is nearly perpendicular to the plane containing Sb, N2 and N3 atoms but not perpendicular to the plane containing Sb, N1 and N4 atoms. Also, Sb-N2

and Sb-N3 bonds [N2-Sb-N3 = 93.40°~90°,] are nearly orthogonal to each other with two phenyl rings on the same side.

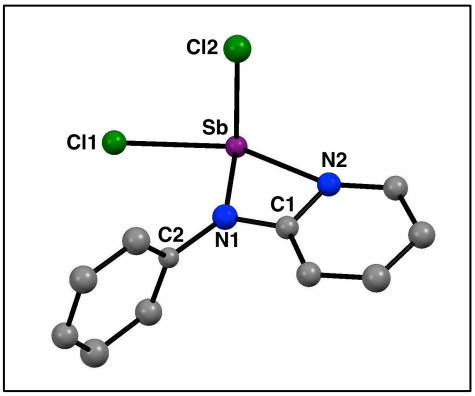

Fig. 2: Molecular structure of **[1]-Cl_2** in ORTEP representation (hydrogen atoms and few carbon labeling are omitted for clarity).

Bond lengths	(Å)	Bond angles	(°)
Sb-Cl1	2.527	Cl1-Sb-Cl2	92.50
Sb-Cl2	2.389	Cl1-Sb-N1	85.43
Sb-N1	2.060	Cl1-Sb-N2	145.40
Sb-N2	2.353	Cl2-Sb-N1	93.50
N1-C1	1.375	Cl2-Sb-N2	90.14
N2-C1	2.353	N1-Sb-N2	59.98
N1-C6	1.423	N1-C1-N2	107.05
		Sb-N1-C1	102.93
		Sb-N2-C1	89.49
		C1-N1-C6	124.72

Table 5: List of specific bond lengths and bond angles of **[1]-Cl_2** molecule in angstrom and degree units respectively.

The **[1]-Cl_2** complex (Fig. **2**) is also an Sb(III) complex with a distorted square pyramidal geometry. In this complex (Fig. **2**), the Sb metal center is possessing four bonds where three are covalent bonds [Sb-Cl1 = 2.527~2.4 Å, Sb-CL2 = 2.389 Å~2.4 Å and Sb-N1 = 2.060 Å~2.033 Å] and one is a coordinate bond [Sb-N2 = 2.353 Å~2.42 Å].[21] On comparing the bond lengths (Table **5**), it is clear that Sb-N1 (2.060 Å) is shorter than Sb-N2 (2.353 Å). The most interesting feature of this complex is that the two Cl atoms (Cl1 and Cl2) are nearly orthogonal to each other [Cl1-Sb-Cl2 = 92.50° ~90°]. Considering the bond angles [Cl1-Sb-Cl2 = 92.50°, Cl1-Sb-N1 = 85.43°, Cl2-Sb-N1 = 93.50°, Cl2-Sb-N2 = 90.14°] of the **[1]-Cl_2** molecule (Table **5**), it is evident that the Sb-Cl1 is nearly perpendicular to the plane containing Sb, Cl2, N1 atoms and Sb-Cl2 is nearly

perpendicular to the plane containing Sb, Cl1, N1 and N2 atoms which in turn depicts the geometry of the complex. Also, it was found that the plane containing the phenyl ring is orthogonal to the plane containing the pyridine ring.

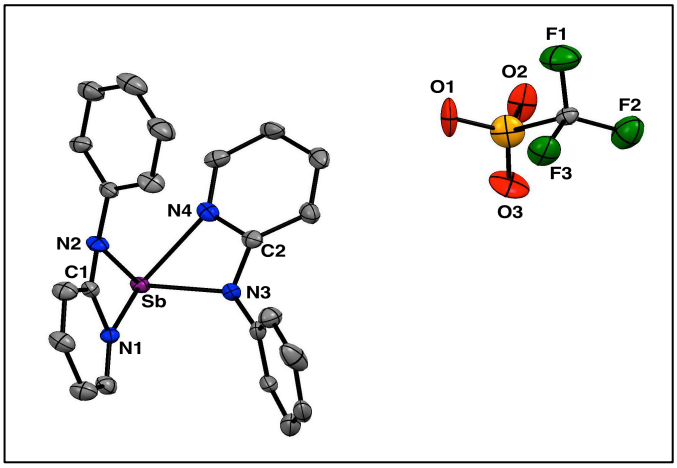

Fig. 3: Molecular structure of **[1]$^{+}$OTf-** in ORTEP representation with 50% displacement ellipsoids as shown (hydrogen atoms and few carbon labeling are omitted for clarity).

Bond lengths	(Å)	Bond angles	(°)
Sb-O1	7.614	N1-Sb-N2	60.47
Sb-N1	2.253	N2-Sb-N4	84.00
Sb-N2	2.109	N3-Sb-N4	60.17
Sb-N3	2.109	N1-Sb-N3	81.64
Sb-N4	2.304	N1-C1-N2	108.98
N2-C1	1.391	N3-C2-N4	108.69
N1-C1	1.346	C1-N2-Sb	98.8
N3-C2	1.357	C2-N4-Sb	92.53
N4-C2	1.339		

Table 6: List of specific bond lengths and bond angles of **[1]$^{+}$OTf-** molecule in angstrom and degree units respectively.

[1]-Cl		[1]$^{+}$ OTf^{-}	
Sb-N1	2.468 Å	Sb-N1	2.253 Å
Sb-N2	2.088 Å	Sb-N2	2.109 Å
Sb-N3	2.087 Å	Sb-N3	2.109 Å
Sb-N4	2.742 Å	Sb-N4	2.304 Å
N1-Sb-N2	53.97°	N1-Sb-N2	60.47°
N3-Sb-N4	58.07°	N3-Sb-N4	60.17°
N1-Sb-N4	74.63°	N1-Sb-N4	125.66°
N2-Sb-N3	93.40°	N2-Sb-N3	94.40°

Table 7: Comparison table between **[1]-Cl** and **[1]$^{+}$OTf-.**

The **[1]$^{+}$OTf-** complex is the cationic species of **[1]-Cl**. From the molecular structure (Fig. **3**), it is clearly evident that the OTf- anionic moiety is discrete from the Sb metal center with Sb-O1 distance of 7.614 Å (Table **6**), which is responsible for enhancing the Lewis acidity of the Sb-center of **[1]-Cl**. On comparing the Sb-N bond lengths of **[1]$^{+}$OTf-** and **[1]-Cl** (Table **7**), it is observed that the Sb-N1 and Sb-N4 (N1 and N4 are nitrogen atoms in the pyridine rings) bonds of **[1]$^{+}$OTf-** have shrunk relatively by ~0.43 Å but the Sb-N2 and Sb-N3 bonds of **[1]$^{+}$OTf-** got negligibly elongated by ~0.021 Å only. And, on comparing the bond angles of **[1]$^{+}$OTf-** and **[1]-Cl** (Table **7**), the angles corresponding to **[1]$^{+}$OTf-** have increased by ~1° but with prominent increase in N1-Sb-N4 angle showing the flipping of the phenyl and pyridine resulting in the two phenyl rings in this complex to be in opposite side unlike in the case of **[1]-Cl**.

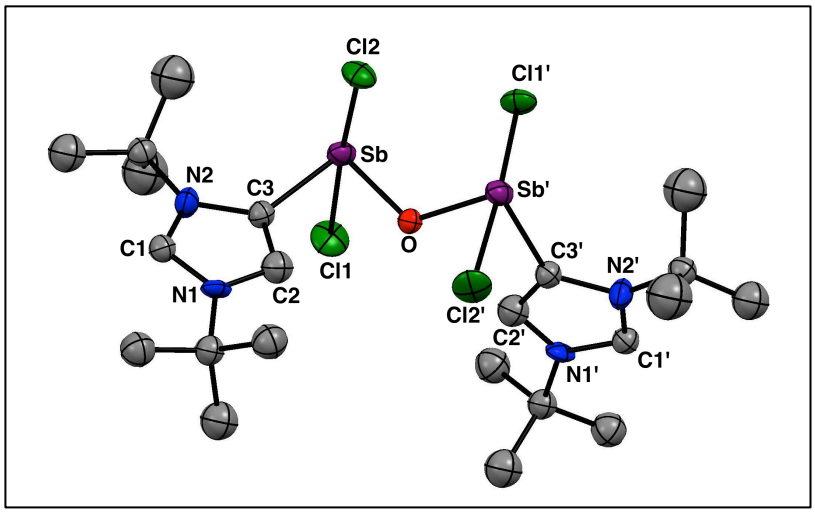

Fig. 4: Molecular structure of obtained **[1]-Cl$_2$-aNHC** in ORTEP representation with 50% displacement ellipsoids as shown (hydrogen atoms and few carbon labeling are omitted for clarity).

Bond lengths	(Å)	Bond angles	(°)
Sb-O	1.958	Sb-O-Sb’	123.10
Sb’-O	1.958	Cl1-Sb-Cl2	175.91
Sb-Cl1	2.616	Cl1’-Sb’-Cl2’	175.91
Sb-Cl2	2.591	Cl1-Sb-O	88.86
Sb’-Cl2’	2.591	Cl2-Sb-O	87.09
Sb2-Cl1’	2.616	Cl1’-Sb’-O	87.09
Sb-C	2.181	Cl2’-Sb2-O	88.86
Sb’-C’	2.181	C-Sb-O	86.15
		C’-Sb’-O	86.15

Table 8: List of specific bond lengths and bond angles of **[1]-Cl$_2$-aNHC** molecule in angstrom and degree units respectively.

The **[1]-Cl_2-aNHC** complex (Fig. **4**) is a symmetric complex in a dimeric form. In observation of the bond lengths and bond angles (Table **8**), it is clearly evident that there is presence of center of inversion about the O atom. Both the Sb metal centres of the molecule possess a see-saw geometry with the nearly linear Cl-Sb-Cl (175.91°~180°) bond. The Sb-O-Sb' (123.10°) bond has a bent configuration bridging the abnormal carbene centers (C3 and C3'). Usually, NHCs are known to exhibit 'normal' binding mode with the metal-centre but sometimes due to various factors NHCs undergo isomerism and tend to exhibit 'abnormal' binding mode with the metal-centre. The factors responsible for the 'abnormal' binding in **[1]-Cl_2-aNHC** are yet to be studied.

4.2 NMR Spectroscopic Evidences:

4.2.1. NMRs of N-phenylpyridine-2-amine, [1]:

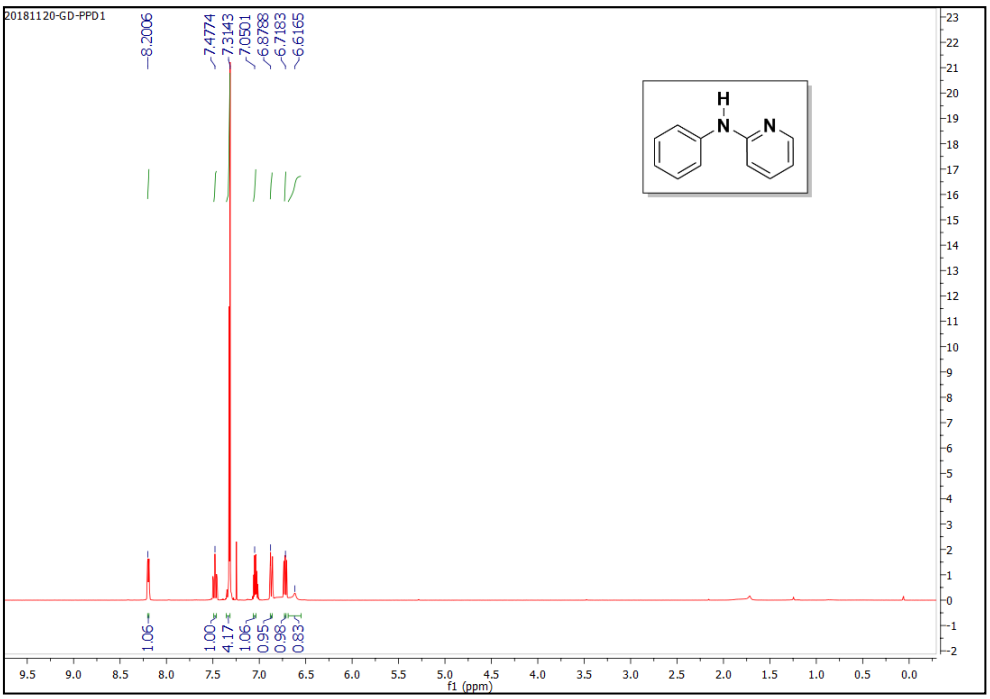

Fig. 5: ^{1}H NMR of N-phenylpyridine-2-amine **[1]** at 400 MHz in $CDCL_3$.

^{1}H NMR (400 MHz, $CDCl_3$, δ, ppm): 6.61 (1H, *br-s*, N**H**), 6.72 (1H, *ddd*), 6.88 (1H, *ddd*), 7.04-7.06 (1H, *m*), 7.31-7.33 (4H, *m*), 7.46-7.48 (1H, *m*), 8.20-8.21 (1H, *m*).

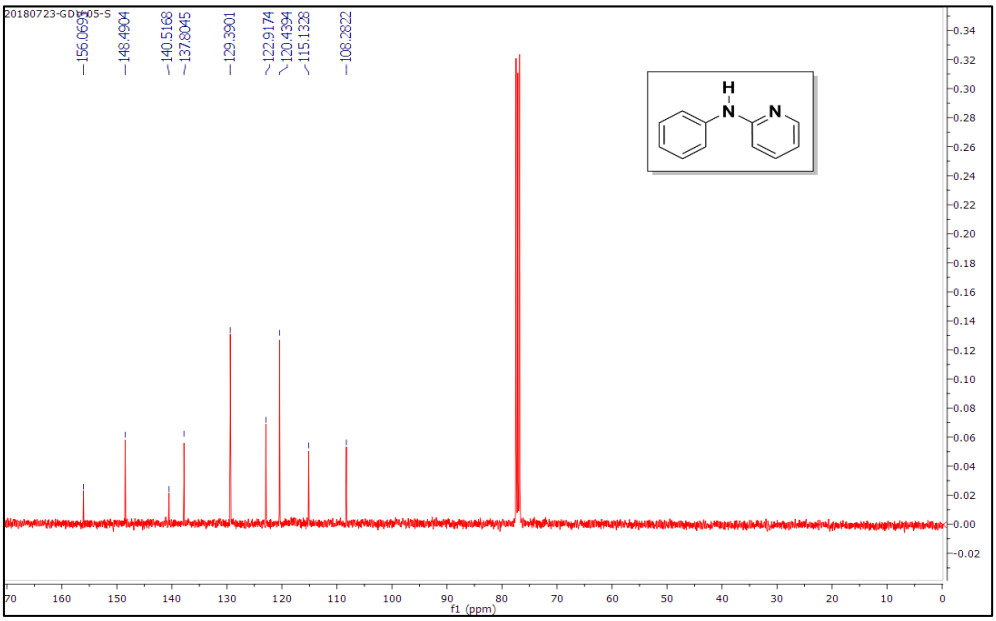

Fig. 6: $^{13}C\{^{1}H\}$ NMR of N-phenylpyridine-2-amine **[1]** at 100 MHz in $CDCL_3$.

$^{13}C\{^{1}H\}$ NMR (100 MHz, $CDCl_3$, δ, ppm): 108.28, 115.13, 120.44, 122.92, 129.39, 137.80, 140.51, 148.49, 156.07.

4.2.2. NMRs of monochloro amino stibane complex, [1]-Cl:

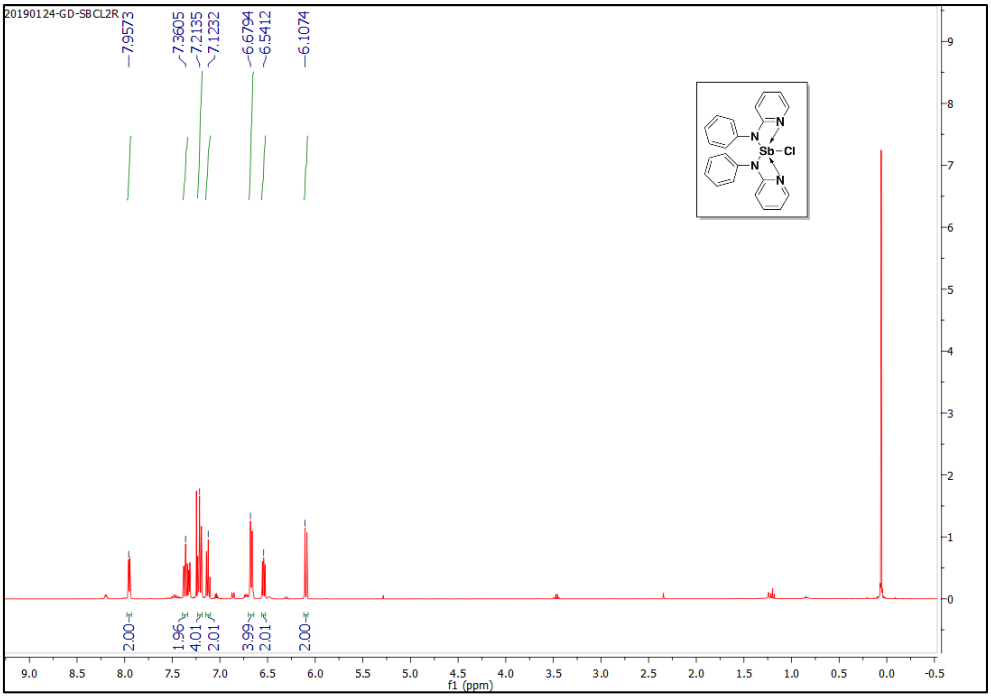

Fig. 7: ^{1}H NMR of monochloro amino stibane complex **[1]-Cl** at 400 MHz in $CDCl_3$.

^{1}H NMR (400 MHz, $CDCl_3$, δ, ppm): 6.11 (2H, *ddd*), 6.54 (2H, *ddd*), 6.68 (4H, *ddd*), 7.12-7.13 (2H, *m*), 7.21-7.22 (4H, *m*), 7.36-7.37 (1H, *m*), 7.95-7.96 (2H, *m*).

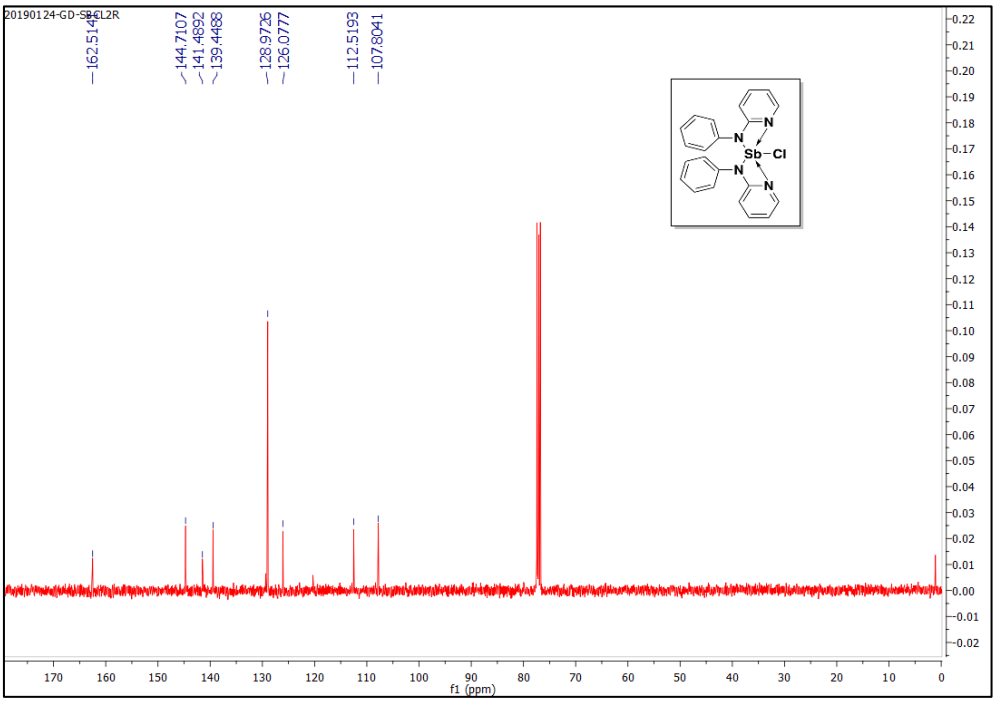

Fig. 8: $^{13}C\{^{1}H\}$ NMR of monochloro amino stibane complex **[1]-Cl** at 100 MHz in $CDCl_3$.

$^{13}C\{^{1}H\}$ NMR (100 MHz, $CDCl_3$, δ, ppm): 107.8, 112.52, 126.07, 128.97, 139.45, 141.49, 144.71, 162.51.

4.2.3. NMRs of dichloro amino stibane complex, [1]-Cl_2:

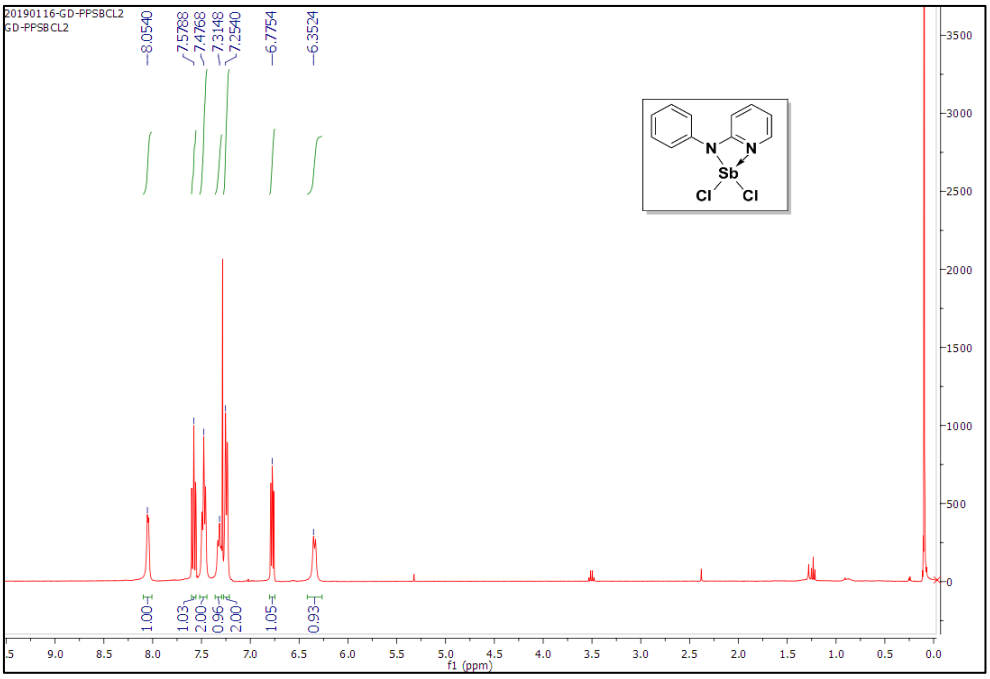

Fig. 9: ^{1}H NMR of dichloro amino stibane complex **[1]-Cl_2** at 400 MHz in $CDCL_3$.

^{1}H NMR (400 MHz, $CDCl_3$, δ, ppm): 6.35 (1H, *ddd*), 6.77 (1H, *ddd*), 7.25-7.27 (2H, *m*), 7.31-7.32 (1H, *m*), 7.47-7.48 (2H, *m*), 7.57-7.58 (1H, *m*), 8.00-8.01 (1H, *m*).

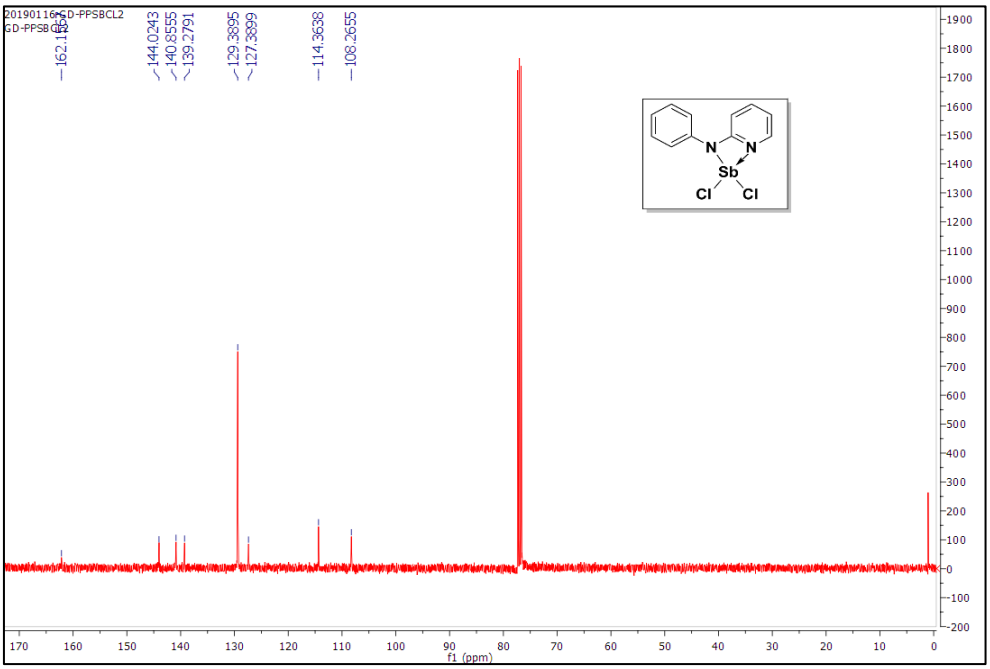

Fig. 10: $^{13}C\{^{1}H\}$ NMR of dichloro amino stibane complex **[1]-Cl_2** at 100 MHz in $CDCL_3$.

$^{13}C\{^{1}H\}$ NMR (100 MHz, $CDCl_3$, δ, ppm): 108.26, 114.36, 127.39, 129.39, 139.28, 140.85, 144.02, 162.15.

4.2.4. NMRs of stibonium cationic complex, $[1]^+$ OTf-:

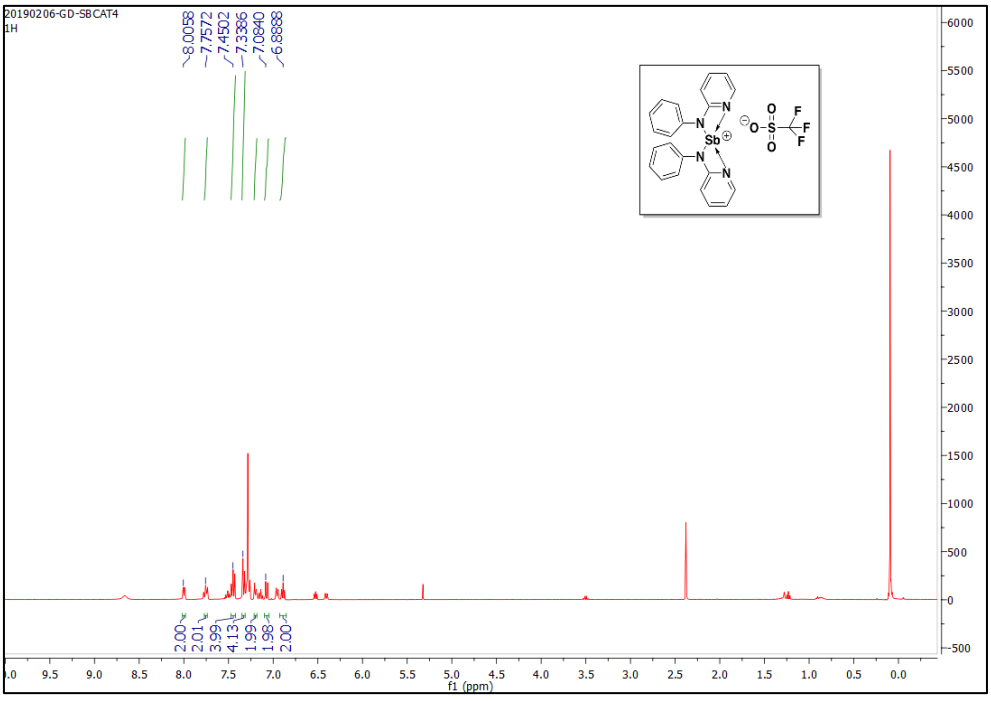

Fig. 11: ^{1}H NMR of stibonium cationic complex **$[1]^+$OTf-** at 400 MHz in $CDCL_3$.

^{1}H NMR (400 MHz, $CDCl_3$, δ, ppm): 6.88 (2H, *ddd*), 7.08 (2H, *ddd*), 7.20-7.25 (2H, *m*), 7.33-7.34 (4H, *m*), 7.45-7.5 (4H, *m*), 7.75-7.76 (2H, *m*), 8.00-8.01 (2H, *m*).

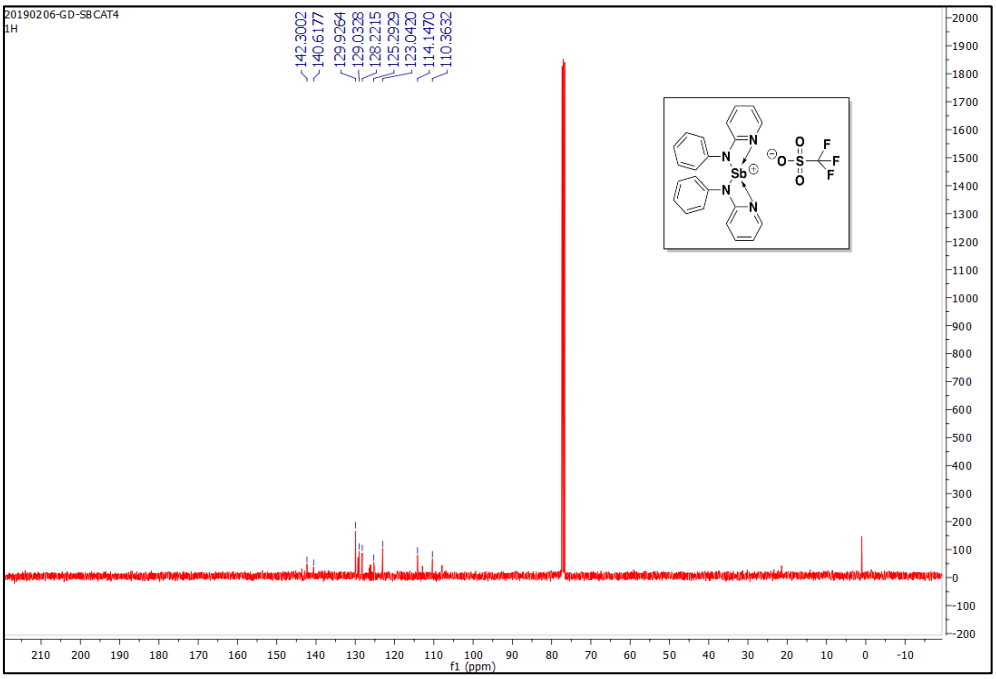

Fig. 12: $^{13}C\{^{1}H\}$ NMR of stibonium cationic complex **[1]$^{+}$OTf-** at 100 MHz in $CDCL_3$.

$^{13}C\{^{1}H\}$ NMR (100 MHz, $CDCl_3$, δ, ppm): 110.36, 114.15, 123.04, 125.29, 128.22, 129.03, 129.93, 140.63, 142.30.

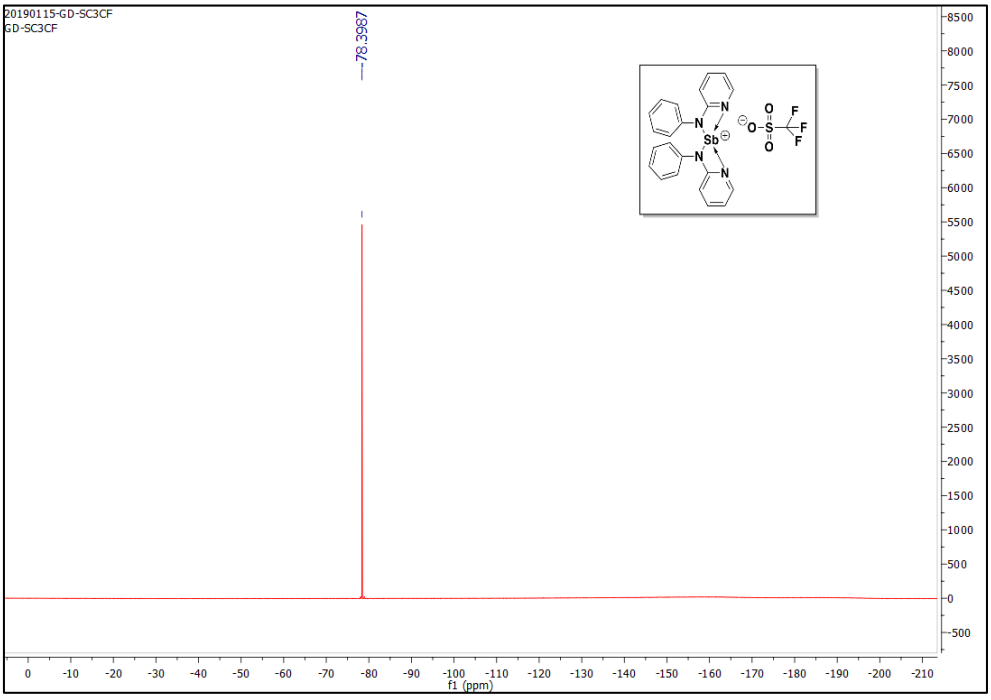

Fig. 13: $^{19}F\{^{1}H\}$ NMR of stibonium cationic complex **[1]$^{+}$OTf-** at 376.6 MHz in $CDCL_3$.

$^{19}F\{^{1}H\}$ NMR (376.6 MHz, $CDCl_3$, δ, ppm): -78.39.

4.2.5. NMRs of obtained abnormal dimer complex, [1]-Cl_2-aNHC:

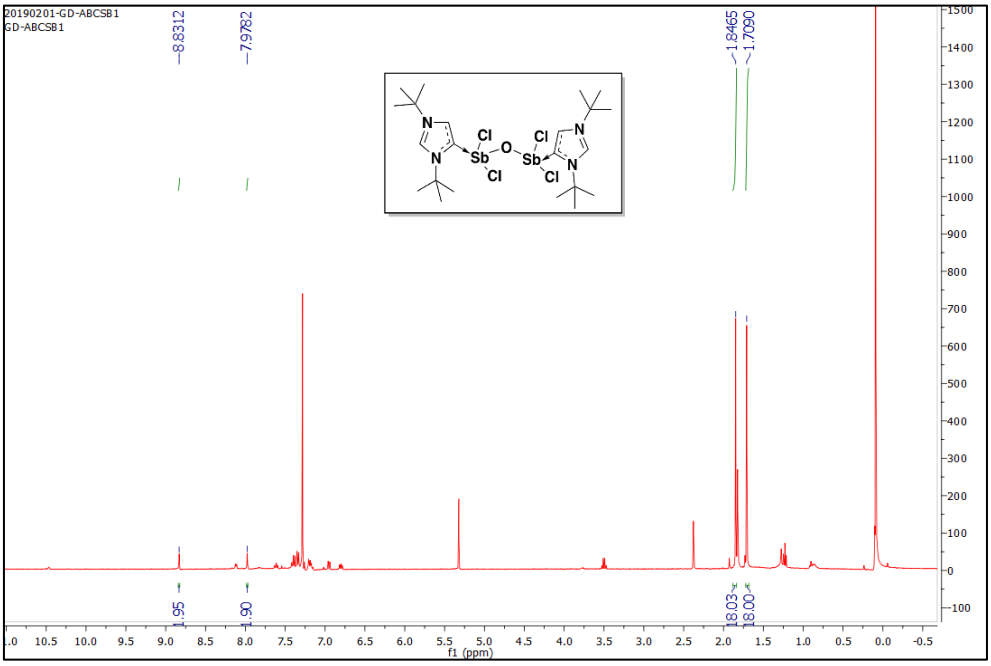

Fig. 14: ^{1}H NMR of the obtained **[1]-Cl_2-aNHC** complex at 400 MHz in $CDCl_3$.

^{1}H NMR (400 MHz, $CDCl_3$, δ, ppm): 1.71 (18H, *s*), 1.84 (18H, *s*), 7.97 (2H, *s*), 8.83 (2H, *s*).

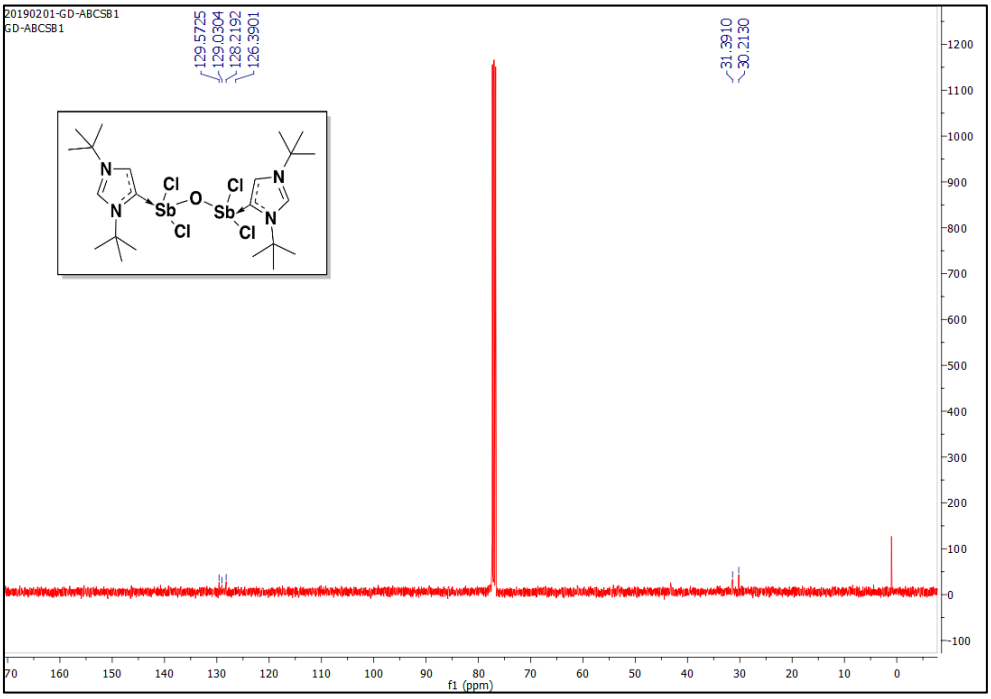

Fig. 15: $^{13}C\{^{1}H\}$ NMR of the obtained **[1]-Cl_2-aNHC** complex at 100 MHz in $CDCL_3$.

$^{13}C\{^{1}H\}$ NMR (100 MHz, $CDCl_3$, δ, ppm): 30.21, 31.39, 126.39, 128.21, 129.03, 129.57.

4.2.6. NMRs of preliminary catalytic reactions with $[1]^{+}OTf^{-}$ as catalyst:

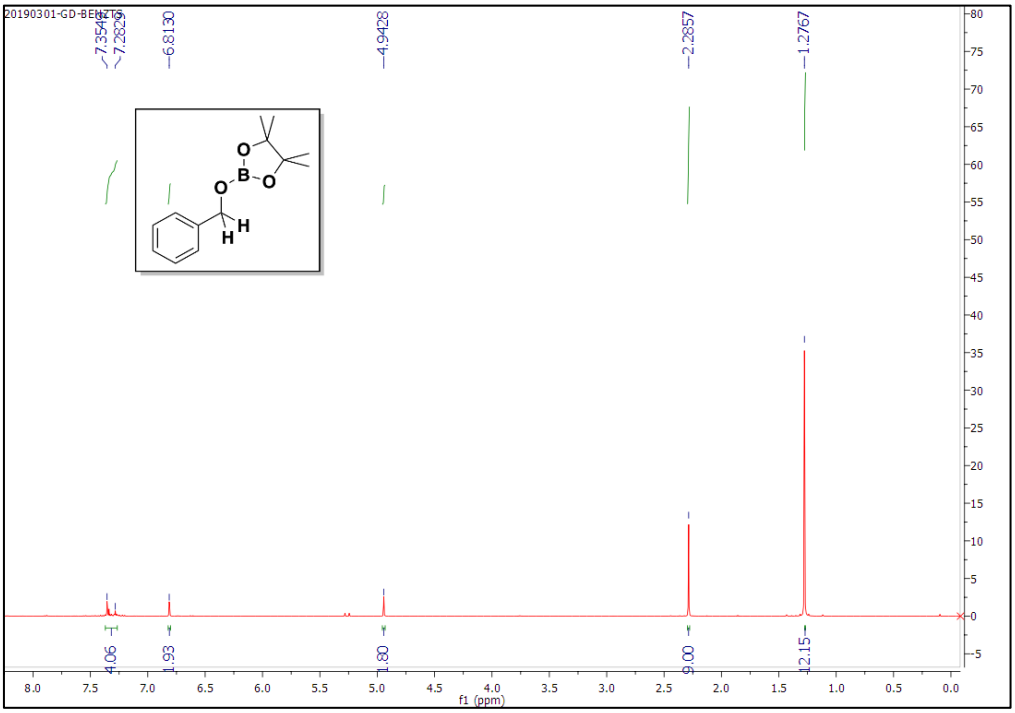

Fig. 16: ^{1}H NMR of the test catalytic reaction of hydroboration with **$[1]^{+}OTf^{-}$** as catalyst at 400 MHz in $CDCl_3$.

^{1}H NMR (400 MHz, $CDCl_3$, δ, ppm): 4.94 (2H, *s*). Calculated yield = (1.8)/2 = 90%.

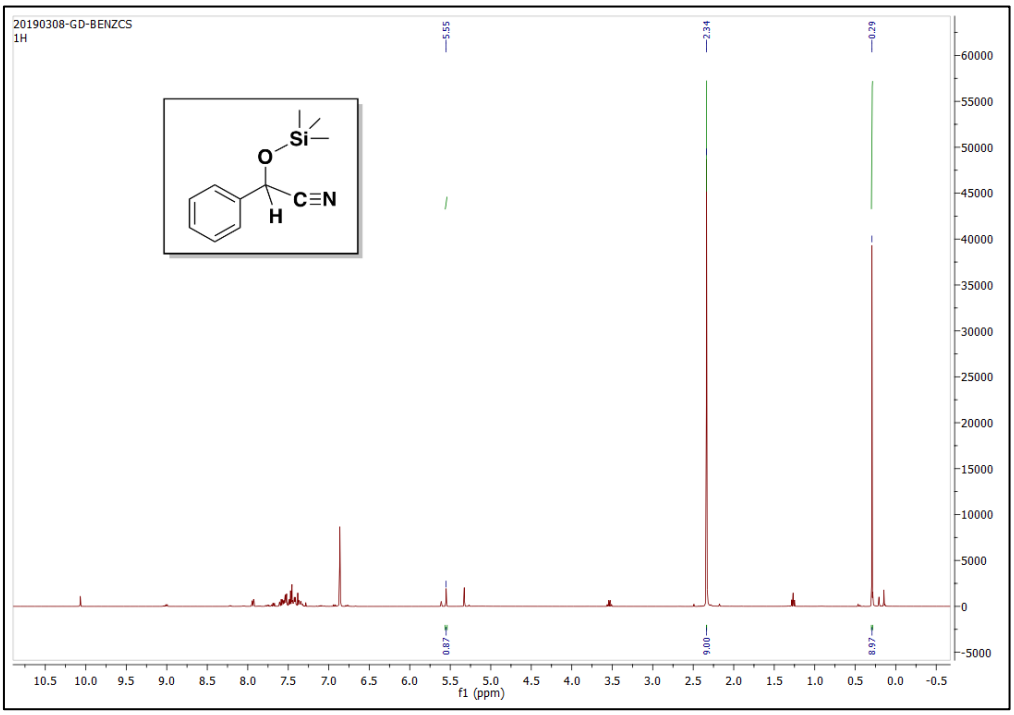

Fig. 17: ^{1}H NMR of the test catalytic reaction of cyanosilylation with **$[1]^{+}OTf^{-}$** as catalyst at 400 MHz in $CDCl_3$.

^{1}H NMR (400 MHz, $CDCl_3$, δ, ppm): 5.55 (1H, *s*). Calculated yield = (0.87)/1 = 87%.

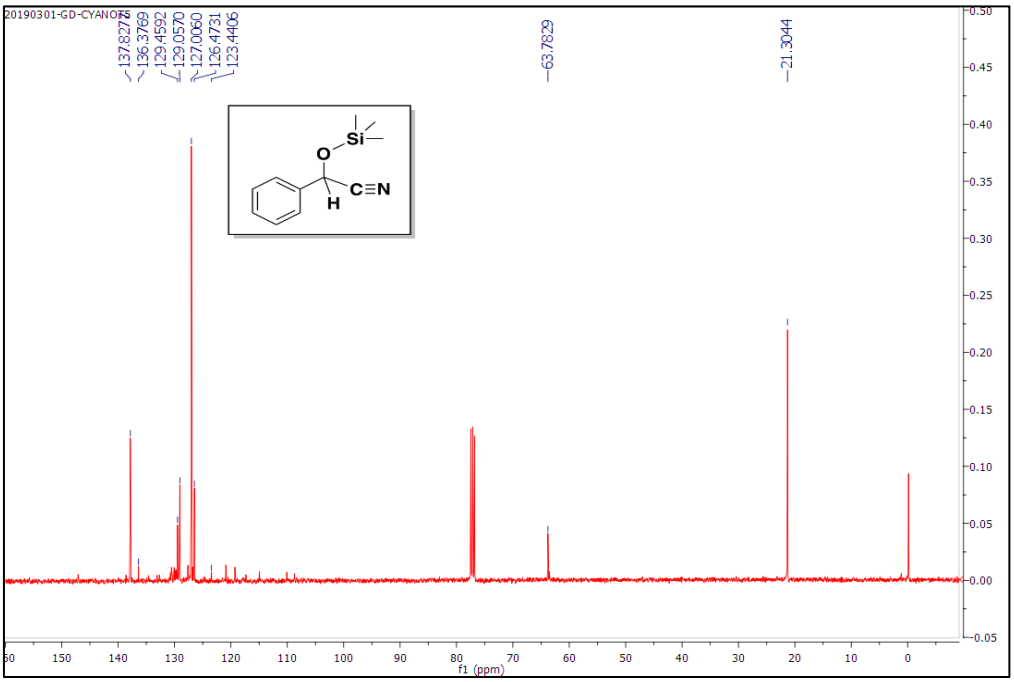

Fig. 18: $^{13}C\{^{1}H\}$ NMR of the test catalytic reaction of cyanosilylation with **[1]$^{+}$OTf^{-}** as catalyst at 100 MHz in $CDCl_3$.

All the NMRs served as supporting information and helped to check the purity of the compounds. The conversion yield% of the catalytic reactions was calculated based on NMR peak integration.

4.3. Mass Spectroscopic evidences:

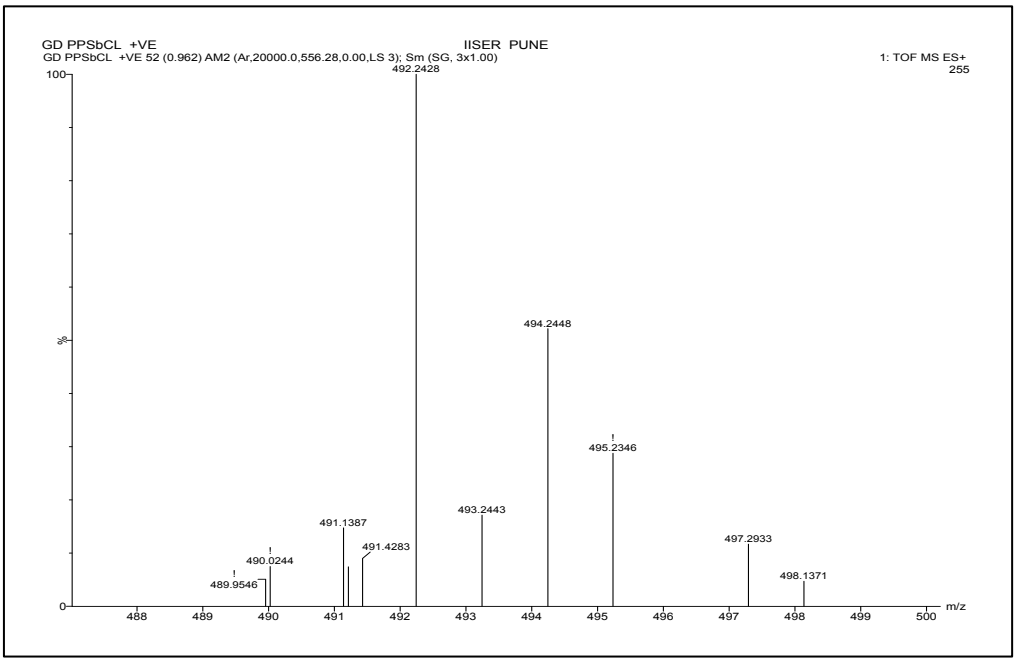

Fig. 19: HRMS spectroscopic data of monochloro amino stibane complex **[1]-Cl** in THF.

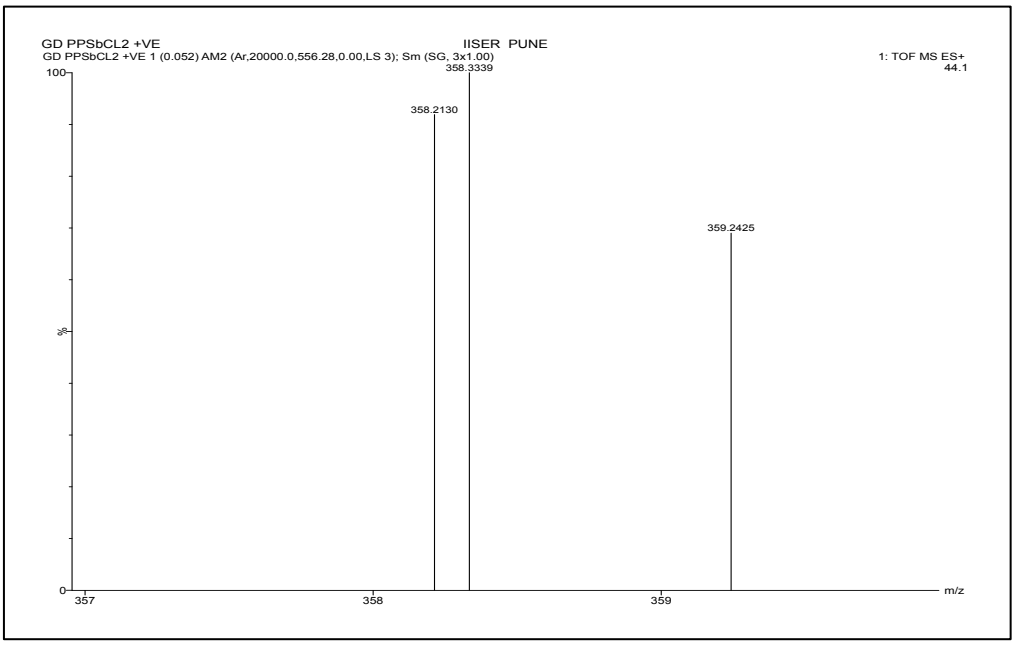

Fig. 20: HRMS spectroscopic data for dichloro amino stibane complex **[1]-Cl_2** in THF.

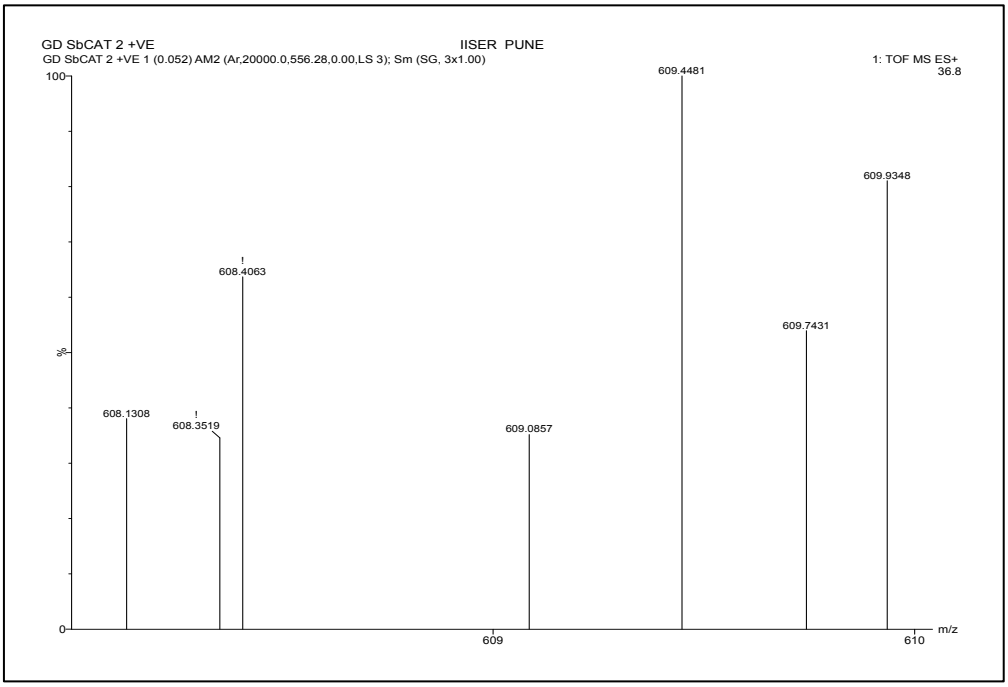

Fig. 21: HRMS spectroscopic data of stibonium cationic complex **[1]$^{+}$OTf-** in THF.

5. Conclusions:

Pnictogen complexes are gathering highlighting attention in the field of organometallic chemistry. Specifically, electron deficient pnictogen complexes are alluring great interest in the field of Lewis acid chemistry. In contribution to this Lewis acid chemistry, in this thesis project we aimed to synthesize stibonium (III) cationic complex, **[1]$^{+}$OTf^{-}** for which we have synthesized two non-reported precursors, monohalo amino stibane complex, **[1]-Cl** and dihalo amino stibane complex, **[1]-Cl$_2$**. By utilizing **[1]-Cl**, we successfully synthesized stibonium (III) cationic species, **[1]$^{+}$OTf^{-}**. Further, we tried to explore the reactivity and catalytic activity of **[1]$^{+}$OTf^{-}**. Unfortunately, most of the reactivity reactions we tried didn't result in the desired product but we observed that **[1]$^{+}$OTf^{-}** is less likely to bind to weak donor like MeCN. Based on the NMR spectroscopic studies of the preliminary catalytic reactions set up for Hydroboration and Cyanosilylation of aldehydes, it is proved that **[1]$^{+}$OTf^{-}** is capable of acting as a catalyst as it resulted in appreciable conversion with yield of 90% and 87% respectively. On the other hand, we also made efforts to generate the cationic species of **[1]-Cl$_2$** but didn't obtain the desired cationic complex. But during this synthetic investigation, we obtained **[1]-Cl$_2$-aNHC** complex, which is different from the desired product yet an interesting species to carry out further studies to investigate the factors that are responsible for the formation of such dimer complex with 'abnormal' binding of NHC and to further predict the possible mechanism pathway.

From this thesis study, it is proved that the synthesized stibonium (III) cationic complex, **[1]$^{+}$OTf^{-}** is capable of acting as a catalyst for both hydroboration and cyanosilylation of aldehydes and this can be further utilized for their thorough catalytic studies, which include optimization of catalyst loading, time standardization and substrate scope. We can also extend its catalytic activity by exploring with other substrates like ketones, alkenes and alkynes. Additionally, we can utilize different NHCs to explore and study the 'abnormal' mode of binding of different carbenes to the metal-centre.

6. References:

1) (a) Olah, G. A.; Schlosberg, R. H., Chemistry in Superacids I. *J. Am. Chem. Soc*., **1968**, *90*, 2726−2727; (b) Olah, G. A.; Klopman, G.; Schlosberg, R. H., Chemistry in Superacids III. *J. Am. Chem. Soc.,* **1969**, *91*, 3261−3268.

2) Pan, B.; Gabbai, F. P., An Air Stable, Lewis Acidic Stibonium salt that Activates Strong Element–Fluoride Bonds. *J. Am. Chem. Soc.*, **2014**, *136*, 9564-9567.

3) Brunet, S., Examples of Catalytic and Selective Routes for Fluorinated Building Blocks. *Org. Process Res. Dev.*, **2014**, *18*, 1067-1071.

4) Ugarte, R. A.; Devarajan, D.; Mushinski, R. M.; Hudnall, T. W.; Antimony(V) cations for the selective catalytic transformation of aldehydes into symmetric ether, α,β -unsaturated aldehydes and 1,3,5-trioxanes; *Dalton Trans.*, **2016**, *45*, 11150-11161.

5) Rao, B.; Chong, C. C.; Kinjo, R., Metal-Free Regio- and Chemoselective Hydroboration of Pyridines Catalyzed by 1,3,2-Diazaphosphenium Triflate. *J. Am. Chem. Soc.*, **2018**, *140*, 652−656.

6) Baba, A.; Fujiwara, M.; Matsuda, H., Unusual cycloaddition of oxiranes with isocyanates catalyzed by tetraphenylstibonium iodide: Selective formation of 3,4-disubstituted oxazolidinones. *Tetrahedron Lett.*, **1986**, *27*, 77−80.

7) Hirai, M.; Cho, J.; Gabbai, F. P.; Promoting the Hydrosilylation of Benzaldehyde by using a Dicationic Antimony-based Lewis acid; Evidence for he Double Electrophilic Activation of the Carbonyl substrate; *Chem. Eur. J.*, **2016**, *22*, 6537-6541.

8) Ugarte, R. A.; Hudnall, T. W., Antimony(V) catalyzed acetalisation of aldehydes: an efficient, solvent-free and recyclable process. *Green Chem.*, **2017**, *19*, 1990–1998.

9) Kobayashi, S.; Komoto, I., Remarkable Effect of Lithium Salts in Friedel-Crafts Acylation of 2-Methoxynaphthalene Catalyzed by Metal Trilates. *Tetrahedron*, **2000**, 56, 6463-6465.

10) Li, N.; Qiu, R.; Zhang, X.; Chen, Y.; Yin, S. F.; Xu, X., Strong Lewis acids of air-stable binuclear triphenylantimony(V) complexes and their catalytic application in C-C bond-forming reactions. *Tetrahedron*, **2015**, *71*, 4275–4281.

11) (a) Mohan, U.; Varshney, A., Copolymerization of Methyl Acrylate with Styrene using Triphenylstibonium 1,2,3,4-tetraphenylcyclopentadieneylide as a Novel Radical Initiator. *Journal of Applied Polymer Science*, **2006**, 1731-1736; (b) Srivastava, S.; Srivastava, A. K., Synthesis and characterization of poly(N-vinyl pyrrolidone) initiated by stibonium ylide. *Designed Monomers and Polymers*, **2006**, *9*, 29-39.

12) Wadey, C. R.; Gabbai, F. P., Fluoride Anion Chelation by a Bidendate Stibonium-Boron Lewis acid. *Organometallics*, **2011**, *30*, 4479-4481.

13) Zhao, H.; Leamer, L. A.; Gabbai, F. P., Anion capture and sensing with cationic boranes: on the synergy of Coulombic effects and onium ion-centred Lewis acidity. *Dalton Trans.*, **2013**, *42*, 8164-8178.

14) Ke, I. S.; Myahkostupov, M.; Castellona, F. N.; Gabbai, F. P., Stibonium ions for the Fluorescence Turn-On Sensing of F^- in Drinking Water at Parts per Million Concentrations. *J. Am. Chem. Soc.*, **2012**, *134*, 15309-15311.

15) Kumar, A.; Yang, M.; Kim, M.; Gabbai, F. P., Lee, M. H., OFF-ON Fluorescence Sensing of Fluoride by Donor-Antimony(V) Lewis acids. *Organometallics*, **2017**, *36*, 4901-4907.

16) Robertson, A. P. M.; Chitnis, S. S.; Jenkins, H. A.; McDonald, R.; Ferguson, M. J.; Burford, N., Establishing the Coordinate Chemistry of Antimony(V) cations: Systematic Assessment of $Ph_4Sb(OTf)$ and $Ph_3Sb(OTf)_2$ as Lewis Acceptors. *Chem. Eur. J.*, **2015**, *21*, 7902-7913.

17) Veith, M.; Bertsch, B.; Huch, V., Zur Element-Stickoff-Doppelbindung in Kationen cyclisher Bis(amino)-phospha, -arsa, -stiba, and –bismutane. *Z. anorg. allg. Chem.*, **1988**, *559*, 73-88.

18) Carmalt, C. J.; Walsh, D.; Cowley, A. H.; Norman, N. C., Cationic complexes of Antimony(III) and Bismuth(III) Stabilized by Intra- or Intermolecular Coordination. *Organometallics*, **1997**, *16*, 3597-3600.

19) Gudat, D.; Gans-Eichler, T.; Nieger, M., Synthesis and unprecedented oxidation of cationic Sb-analogue of an Arduengo's carbene. *Chem. Commun.*, **2004**, 2434-2435.

20) Burford, N.; Cameron, T. S.; Macdonald, C. L. B.; Robertson, K. N.; Schurko, R.; Walsh, D., Dissociation of 2,4-Bis(2,4,6-tri-tert-buylphenyl)-cyclo-1,3,-dipnicta-2,4-diazanes (pnict = P, As, Sb) Imposed by Substituent Steric Strain: A Cyclobutane/Olefin Analog. *Inorg. Chem.*, **2005**, *44*, 8058-8064.

21) Hering, C.; Lehmann, M.; Schulz, A.; Villinger, A., Chlorine/ Methyl Exchange Reactions in Silylated Aminostibanes: A New Route to Stibinostibonium Cations. *Inorg. Chem.*, **2012**, *51*, 8212-8224.

22) Price, J. T.; Lui, M.; Jones, N. D.; Ragogna, P. J., Group 15 Pnictenium Cations Supported by a Conjugated Bithiophene Backbone. *Inorg. Chem.*, **2011**, *50*, 12810-12817.

23) (a) Bourget-Merle, L.; Lappert, M. F.; Severin, J. R., The Chemistry of β-Diketiminatometal Complexes. *Chem. Rev.*, **2002**, *102*, 3031-3065; (b) Burford, N.; D'eon, M.; Ragogna, P. J.; McDonald, R.; Ferguson, M. J., Synthesis and Structures of complexes demonstrating the Coordinate versatility of the 2,4-diimino-3-phosphinopentene Anion (γ-phosphino β-

diketiminate). *Inorg. Chem.*, **2004**, *43*, 734-738.

24) Lin, B.; Liu, M.; Ye, Z.; Ding, J.; Wu, H.; Cheng, J., Copper-TBAF catalyzed arylation of amines and amides with aryl trimethoxysilane. *Org. Biomol. Chem.*, **2009**, *7*, 869-873.

25) Arnold, P. L.; Pearson, S., Abnormal N-heterocyclic carbenes. *Coord. Chem. Rev.*, **2007**, *251*, 596-609.

26) Water. J. B.; Chen, Q.; Everitt, T. A.; Goicoehea, J. M., N-heterocyclic carbene adducts of the heavier group 15 tribromides. Normal to abnormal isomerism and bromine ion abstraction. *Dalton Trans.* **2017**, *46*, 12053-12066.